TENSILE PROPERTIES OF GLASS-FABRIC LAMINATES WITH LAMINATIONS ORIENTED IN ANY WAY

No. 1853

November 1955

Information Reviewed and Reaffirmed 1960

This Report is One of a Series
Issued in Cooperation with the
ANC-17 PANEL ON PLASTICS FOR AIRCRAFT
of the Departments of the
AIR FORCE, NAVY, AND COMMERCE

FOREST PRODUCTS LABORATORY
MADISON 5, WISCONSIN

UNITED STATES DEPARTMENT OF AGRICULTURE
FOREST SERVICE
In Cooperation with the University of Wisconsin

TENSILE PROPERTIES OF GLASS-FABRIC LAMINATES WITH LAMINATIONS ORIENTED IN ANY WAY[1]

By

E. C. O. ERICKSON, Engineer
and
C. B. NORRIS, Engineer

Forest Products Laboratory,[2] Forest Service
U. S. Department of Agriculture

Abstract

A mathematical analysis of the elastic properties of glass-fabric-base laminates in the plane of the laminate is presented. This analysis provides a theoretical means of determining the mechanical properties at any angle in the plane of the laminate, based on the orientation and basic properties of the individual orthotropic laminations. Comparisons between computed and experimental verification values in tension are presented for two laminates composed of the same fabric and for one laminate combining three different fabrics.

Introduction

More efficient means of utilizing present-day glass-fabric-base laminates in structural applications for aircraft are now available. Previous studies have indicated that strength properties may be varied by varying the orientation of the laminations, or by combining laminations

---

[1] This progress report is one of a series (ANC-17, Item 54-1) prepared and distributed by the Forest Products Laboratory under U. S. Navy Bureau of Aeronautics Order No. NAer 01610 and U. S. Air Force No. DO(33-616) 53-20, Amend. A2(55-295). Results here reported are preliminary and may be revised as additional data become available.

[2] Maintained at Madison, Wis., in cooperation with the University of Wisconsin.

of differing mechanical properties within the laminate. The purpose of this report is to present and experimentally verify a mathematical analysis of the elastic and strength properties of a laminate made of laminations oriented in any desired way by testing three laminates, one of which is orthotropic and the other two aeolotropic.

Each of six test panels made by the Forest Products Laboratory for this study were laminated from 38-inch squares of finish 114[3] fabric. Three of these panels were parallel laminated and were tested to provide data upon which the computations could be based. The laminations in the other three panels were oriented in a way that seemed likely to best illustrate the usefulness of the analysis.

The load-deformation curves obtained by test presented a choice of elastic moduli. Four such choices were made for each specimen tested whenever such choices were possible. The values obtained by these choices from the control panels were substituted in the equations of the mathematical analysis to obtain computed values comparable to those obtained from tests of the other panels.

Materials and Fabrication

Materials

Three types of glass fabrics were used in this study, namely 181-114, 143-114, and 162-114. Type 181-114 is a satin-weave fabric of approximately equal strength in the warp and fill direction. Type 143-114 is a unidirectional weave fabric with a warp-to-fill strength ratio of about 8 to 1. The 162-114 fabric has a warp-to-fill strength ratio of about 3 to 2. The laminating resin, identified as batch No. 884, was a high-temperature-setting, low-viscosity resin of the polyester (styrene-alkyd) type, known as laminating resin 2.

---

[3] Finish 114 fabrics were approved for use in this study in order to make use of materials already on hand. These fabrics will not conform to the wet-condition requirements of glass fabrics now specified for aircraft laminates, but will conform to the standard dry-condition requirements of Specification MIL-P-8013. As such, they are considered satisfactory for these experimental tests made solely to verify the mathematical analysis of laminates with random orientation of laminations. Since the study involves only tests made in the dry condition and comparisons of test results with computed results, the validity of the conclusion is in no way affected by the use of fabrics with this finish.

Fabrication

Six test panels, each approximately 1/8 inch by 36 by 36 inches, were made at essentially the same time, using a fresh batch of the same resin. The fabric and resin were laid up between cellophane-covered cauls. Each sheet of fabric was grasped at its four corners and carefully tensioned to bring the fill threads at 90° to the warp weave before it was finally positioned on the assembly caul. A paperboard template considerably larger than the cauls was placed under the bottom caul before assembly. Several groups of parallel grid lines had been scored upon the template, parallel to the several angles of orientation desired in the test panels. The template enabled two assembly men to orient the warp direction of each sheet as nearly parallel to the desired direction with respect to the chosen axis of reference of each panel as it was possible to aline them by eye, before lowering the sheet into position upon the previously positioned adjacent sheet and freshly spread resin. A considerable effort was made during layup to get a good distribution of resin, thoroughly wet all threads, and work out the air entrapped between plies. Minor flaws, such as surface wrinkles, were present in some panels. The specimens were so chosen, however, that there were no noticeable imperfections in the critical sections.

Each panel was cured in a hot press for 20 minutes at 220° F., followed by 70 minutes at 250° F. Curing pressures, resin content, and general information on each panel are presented in table 1.

Two of three panels (Nos. 4 and 5) designed for comparison with computed properties were composed of the same fabric, whereas three different fabrics were combined in panel No. 6. Panel No. 4 consisted of 12 plies of 143-114 fabric, laid up with the warp direction of 6 parallel alternate laminations at an angle of 30° to the warp direction of 6 parallel adjacent laminations. Thus the natural axis of the laminate (which was chosen to be the axis of reference) fell midway between the natural axis of each parallel group of six laminations.

Panel 5 consisted of 13 laminations of 143-114 fabric with the warp direction of three groups of laminations parallel and oriented as follows: The laminations were numbered consecutively from 1 to 13; laminations Nos. 1, 2, 4, 5, 7, 9, 10, 12, and 13 were laid up with the warp direction parallel to the axis of reference; laminations Nos. 3 and 11 making an angle of 110°; and laminations Nos. 6 and 8 making an angle of 140° with the same axis. The angles were measured positively in a counterclockwise direction from the arbitrary axis of reference.

The 12 laminations of panel 6 included 3 of fabric 162-114, 4 of 143-114, and 5 of 181-114. The warp direction of each fabric was parallel and was oriented as follows: Laminations 1, 6, and 12 were of 162-114 fabric and were laid up with their warp direction making an angle of 0° to an axis of reference; laminations 3, 5, 8, and 10 were of 143-114 fabric making an angle of 10°; and laminations 2, 4, 7, 9, and 11 were of 181-114 fabric making an angle of 140° to the same axis. The angles were measured positively in a counterclockwise direction.

Three panels for test determinations of basic properties of each fabric were parallel laminated with the warp direction of all laminations parallel to the axis of reference. Panels Nos. 1 and 2 consisted of 12 laminations each of fabrics 143-114 and 181-114, respectively. Panel No. 3 consisted of eight laminations of 162-114 fabric.

Test Specimens

The location and direction of test specimens with respect to the trimmed edges, warp direction of laminations, and axis of reference of the panels are indicated in the cutting diagrams, figures 1, 2, and 3.

Nine tensile specimens were taken parallel, 9 perpendicular, and 9 at 45° to the warp direction from each of the three parallel-laminated control panels (fig. 1). The axis of reference was taken parallel to the warp direction, so that these directions are referred to as 0°, 90°, and 45°. Six tensile specimens from among those having the 0° warp direction and 6 from among those having the 90° warp direction (numbered 1, 3, 4, 6, 7, and 9) were used for tensile tests, and the 3 remaining 0° and 90° specimens (numbered 2, 5, and 8) were used for the determination of Poisson's ratios. Three compression specimens were taken from the 0° and 90° directions of each of the control panels (fig. 1).

Three tension specimens were taken from panels 4, 5, and 6 in each of the several directions, as shown in figures 2 and 3.

Each tensile specimen was 16 inches long by 1-1/2 inches wide before it was shaped. Each was reduced at the center of its length to a minimum section 0.8 inch wide and 2-1/2 inches long, which was connected to the maximum end sections by circular arcs of 20-inch radius, tangent to the minimum center section. Tension specimens were cut to approximate size on a bandsaw, and finished to the desired shape and curvature by use of an emery wheel mounted on a shaper head.

Compression specimens 1 inch wide and 4 inches long were cut to size with a 1/8-inch emery wheel rotated at 1,770 revolutions per minute in the arbor of a variable-speed table saw. Square, smooth edges were obtained by this method of cutting.

All specimens were conditioned to approximately constant weight at 75° F. and 50 percent relative humidity before test. Specimens were tested under controlled conditions of 75° F. and 64 percent relative humidity, but exposed to these conditions for as short a time as possible.

Test Methods

Tension Tests

All tensile-type specimens were held in Templin-type grips and tested in a hydraulic testing machine (fig. 4). Load was applied at a head speed of 0.035 inch per minute. The first tensile specimen of each test-direction group was tested directly to failure in one continuous operation. The remaining tension specimens in each group were first loaded to a load almost equal to the secondary proportional limit load as determined from the load-deformation curve of the first specimen of the group. Specimens were then unloaded back to the initial load point, after which they were immediately reloaded under a continually increasing load until failure occurred. Load deformation data were recorded at convenient increments of load during the initial loading, the unloading, and the reloading operations. This loading cycle was used on all tensile specimens unless otherwise noted.

Data for the determination of Poisson's ratios were obtained from tensile-type specimens held in Templin grips. Each specimen was loaded and unloaded 4 times in one continuous operation at a rate of 0.035 inch per minute. The first 2 loading runs were carried up to a load of about three-fourths of the secondary proportional limit load of the material, as previously determined from the initial tensile tests, before unloading. The third and fourth loading runs were continued to the secondary proportional limit load before unloading. Once testing was begun, the specimens were not completely unloaded until after the fourth and final unloading run. Each of these specimens was loaded and unloaded in a continuous operation without any intentional rest or recovery periods.

Deformation data for specimens from panels 1 to 4 inclusive were obtained parallel to the applied load only. Strains were measured in the stress direction across a 2-inch gage length with a pair of Marten's mirrors reading to 0.00001 inch.

Strains for Poisson's ratio determinations from tensile-type specimens of panels 1 to 3, inclusive, were measured with SR-4 metalectric strain gages reading to 0.000001 inch. Gages of 1-inch and 1/2-inch gage length were applied to each side of each specimen at the net section, the 1-inch gages parallel and the 1/2-inch gages perpendicular to the direction of stress.

Strains of the experimental specimens from panels 5 and 6 were measured with metalectric strain gages of the 45° Rosette-type gage (AR-7) having three elements at 0°, 45°, and 90° to the first element. These gages were applied in pairs directly opposite each other, one on each side of the specimen, with the two 45° elements always in the same plane. No particular difficulty was experienced in using these gages, except as follows: A few gages loosened before testing began and had to be reglued. Approximately 1 specimen in each like group of 3 had the 45° elements oriented at 90° to those of the 2 other specimens. This circumstance necessitated the use of individual rather than average experimental values in comparing these 45° stress-strain ratios with computed values.

Compression Tests

Compression specimens were loaded on their squared ends and were restrained from buckling by an apparatus similar to that shown under Method No. 1021.1 of Federal Specification L-P-406b for Plastics, Organic. Load was applied at a head speed of 0.012 inch per minute, and strains were measured across a 2-inch gage length with a pair of Marten's mirrors.

Method of Obtaining Experimental Data

Experimental load-deformation data obtained from each tensile test were plotted at convenient scales, and curves were drawn. Most of these specimens exhibited the usual two straight-line sections common to parallel-laminated tensile specimens at 0° and 90° to the warp direction and normally referred to as initial and secondary. Only the 0° specimens of the unidirectional fabric 143-114 in panel 1 failed to develop a definite second straight-line portion in all six test specimens. In all other instances at 0° and 90°, a full complement of six initial values of modulus of elasticity and stress at proportional limit, based on the initial straight-line portion of the load-deformation curve, was obtained, together with six secondary values based on the second straight-line portions.

Perhaps unique among tests of this kind was the procedure of recording load-deformation data during each unloading, after the secondary proportional limit load was reached, and during the subsequent reloading to failure. Each of these plots exhibited definite straight-line portions and each such portion, beginning at the initial loading increment, was used to obtain the respective unloading and reloading values. Thus there were 4 slopes recorded, 1 from each phase of the loading cycle. These slopes are referred to as the initial, secondary, unloading, and reloading slopes.

Representative load-deformation curves for the 0°, 90°, and 45° tension specimens from the 143-114 and 162-114 fabrics used in panels 1 and 3, respectively, are shown in figures 5 through 10. The load-deformation curve of the first specimen loaded directly to failure is shown, for purposes of comparison, adjacent to a companion specimen whose initial loading was interrupted shortly after a secondary proportional limit load was reached. Secondary load-deformation phases were not obtainable from the 45° specimens, so all of the 45° specimens were loaded directly to failure. Load deformation curves of the 181-114 fabric in panel 2 were quite similar to the curves of the 162-114 fabric in panel 3, shown in figures 8, 9, and 10.

A few representative load-deformation curves from tests of specimens taken from panels 5 and 6 at various angles to the arbitrary axis of reference are shown in figures 11 through 15. Load-deformation curves obtained from each of the three elements of the Rosette-type strain gage are shown in adjacent plots for ready comparison of the behavior characteristics of the 0° (vertical) element, the 90° (horizontal) element, and the 45° element of the Rosette gages. The vertical element of the Rosette gage was always parallel to the direction of applied stress.

In general, the 0° and 90° gage elements gave fairly consistent results among similar specimens. Contrarywise, the strain data obtained from the 45° element of the gages were very inconsistent. A number of the 45° gages first registered tension and later compression during the same loading phase. The 45° curves of specimens 150°-5-1 and 150°-5-3, shown in figure 12, illustrate such a condition and make obvious the reason why only the initial load-strain phase of the data could be used.

Similar load-deformation curves were plotted from data from the vertical and horizontal gages of the 0° and 90° specimens tested for Poisson's ratios. Only ratios of the slopes of the first 2 of 4 loading runs were used in calculating Poisson's ratios.

Presentation of Data

Experimental Data

Experimental values obtained from the tests are presented in tables 2 through 7.

Table 2 presents the results of tension tests with the stress applied at an angle of 0°, 90°, and 45° to the direction of the warp of parallel-laminated panels 1, 2, and 3. Maximum, minimum, and average values of modulus of elasticity are given for each of the four phases of load-deformation cycles, together with corresponding values of proportional limit stress and ultimate strength. Values of the modulus of rigidity associated with the 0° and 90° axes (G_{0-90}) computed by means of equations (14) of the Appendix and the experimental values in this table and in table 4 are also given.

Table 3 presents the results of compression tests with stress applied in the 0° and 90° directions with respect to the warp of the parallel-laminated panels 1, 2, and 3. Individual and average values of modulus of elasticity, stress at proportional limit, and ultimate strength are given.

Table 4 presents individual and average values of Poisson's ratios from tensile-type tests with stress applied in the 0° and 90° directions with respect to the warp of the laminations in panels 1, 2, and 3. As far as possible, ratios were calculated for each of the 3 laminates in each of the 4 phases of the loading cycle.

Table 5 presents the results of tensile tests of panel 5 with the stress applied at various angles to an arbitrary axis of reference (fig. 3). Values of ultimate strength and stress-strain ratios for individual specimens are given. Values of stress-strain ratios in the 0°, 90°, and 45° directions with respect to the direction of applied stress are presented. Values are shown for as many of the 4 phases of the loading cycle as were possible from the data obtained.

Table 6 presents corresponding tensile test data from panel 6 in the same form as presented in table 5.

Table 7 presents the results of tensile tests with stress applied at 0°, 90°, and 45° to the axis of reference of the orthotropic panel, No. 4 (fig. 2). Presented also in this table are the corresponding theoretical values computed for comparison with the experimental values.

Computed Data

Computed values of strength and elastic moduli corresponding to the experimental test values of panels 4, 5, and 6 are presented in tables 7 through 11. The computed values presented in these tables were obtained in accordance with the mathematical analysis presented in the Appendix. The elastic properties obtained from panels 1, 2, and 3 for each of the 4 phases of the loading cycle were substituted in the equations of the Appendix to obtain corresponding computed values for the 4 phases of the loading cycle for panels 4, 5, and 6. Using these values, 4 corresponding values for tensile strength were computed.

The computed values of elastic moduli presented in table 7 for panel 4 were obtained in accordance with section 7 of the Appendix. Computed strength values for this panel were determined by means of the equations of section 6.

Tables 8 and 9 present the computed values of stress-strain ratios for comparison with corresponding experimental values from specimens of panels 5 and 6 respectively. Stress-strain ratios in the 0°, 90°, and 45° directions with respect to the lengths of the specimens cut at various angles to the axis of reference are given for each of the 4 phases of the loading cycle. Values of the ratios at both plus and minus 45° were computed so that they could be compared with the particular experimental values obtained. These stress-strain ratios were computed according to section 5 of the Appendix.

Tables 10 and 11 present computed values of tensile strength for comparison with experimental strength values of specimens from panels 5 and 6. These computed values were obtained in accordance with the equations presented in section 6 of the Appendix. The elastic properties computed from each of the 4 phases of the loading cycle were used; thus, 4 computed strength values were obtained. Section 6 of the Appendix yields a strength value associated with each lamination of the laminate. Thus, the computed strength values for panel 5 are each an average of 13 such values, and those for panel 6 are each an average of 12 such values. These averages are weighted according to the relative thicknesses of the individual laminations.

Figures 16 through 21 show, with one exception, curves of computed stress-strain ratios and corresponding experimental values for the four phases of the loading cycles for specimens taken from panels 5 and 6. In most of these figures, the computed values are connected by a smooth curve.

The experimental values were taken from tables 5 and 6 and the computed values from tables 8 and 9. Experimental values in the stress direction (0°) and perpendicular to the stress direction (90°) are, in each case, the average value for each group of 3 test specimens at the respective test angles and loading-cycle phase. Experimental values at 45° are in each case individual values, because the values measured at plus 45° could not, of course, be averaged with those measured at minus 45°. The plots of these values are divided into 2 halves. Stress-strain ratios at plus 45° are plotted on the left half and those at minus 45° on the right half.

Corresponding computed and experimental strength values for specimens from panels 5 and 6 are presented in figure 22. Experimental values are indicated by solid circles and computed values by open circles. A smooth line has been drawn through the plotted points representing computed values for the initial phase. Plotted points for each of the other loading-cycle phases are also shown clustered around each corresponding initial value. The experimental strength values were taken from tables 5 and 6, and the computed values from tables 10 and 11.

Analysis of Data

Inspection of table 7 and figures 16 through 22, which show the degree of agreement between the theoretical and experimental values, leads to the following observations.

The computed values of the stress-strain ratios for panel 4 agree very well with the experimental values in all but the secondary phase of the loading cycle, as shown in table 7. Thus if initial, unloading, or reloading values of elastic properties are used in the equations of the mathematical analysis, reasonably good estimates of the related moduli of elasticity of panel 4 are obtained.

Figure 16 shows similar data for panel 5 and figure 19 for panel 6. Reasonable agreement between computed and experimental values is indicated.

Figure 17 shows the stress-strain ratios associated with Poisson's ratios for panel 5. Good agreement between the computed and experimental values is obtained only for the initial phase of the loading cycle. Only general agreement is obtained for the reloading phase and poor agreement for the other two phases.

Similar information is given for panel 6 in figure 20. Again good agreement between the computed and experimental values is obtained only for the initial phase. Values for the secondary phase were not plotted because they were too erratic. The computed values for the other two phases give only rough, unconservative estimates of the experimental values.

Figure 18 shows stress-strain ratios at plus and minus 45° for panel 5 and figure 21 those for panel 6. The computed curves for the secondary phase of the loading cycle are quite different from the computed curves for the other phases. The experimental values for this phase do not agree well with the computed values. The agreement between the computed and experimental values for the other phases seems reasonable when it is remembered that individual rather than average values are plotted.

Figure 22 shows the tensile strength values for panels 5 and 6, respectively. Computations of tensile strength based on elastic properties obtained from each of the four phases lead to substantially the same results. The computed tensile strength values are slightly conservative.

Conclusions

1. The mathematical analysis of elastic properties is not applicable to the secondary phase of the loading cycle.

2. The mathematical analysis for the elastic properties is in reasonable agreement with experimental values in the initial, unloading, and reloading phases. The best agreement was obtained in the initial phase.

3. The mathematical analysis provides an excellent estimate of tensile strength regardless of the loading-cycle phase used in the determination of the elastic properties. The values obtained from the secondary phase, however, are the least reliable.

APPENDIX

Mathematical Analysis

The first four sections of this appendix are taken from the material in Chapters 1, 2, 3, and 6 of "The Mathematical Theory of Elasticity," by A. E. H. Love but are restricted to two dimensions. This restriction greatly simplifies the mathematical expressions, so that they can be written in algebraic forms without being unduly cumbersome.

The fifth section of this Appendix applies this theory to laminates made of aeolotropic laminations and closes with the special case of orthotropic laminations.

The sixth section derives equations for the strength of laminates made of orthotropic laminations -- more particularly, those laminations made of fabric or veneer. This derivation is based on the previous sections and on some previously reported work of the Forest Products Laboratory.

Sections 7 and 8 deal with the special cases of a laminate made of two identical orthotropic laminations arbitrarily orientated with respect to each other, and of a laminate made up of a number of different orthotropic laminations having their natural axes parallel to each other.

1. Transformation Equations for Stress and Strain

Consider a sheet of material subjected to uniformly distributed loads applied at its edges and acting in the plane of the sheet. The stresses and strains in the sheet are referred to the orthogonal axes x and y or to the orthogonal axes ξ and η. The x axis makes an angle θ with the ξ axis, which is measured positively counterclockwise from the ξ axis to the x axis (fig.23). The stresses are f_x, f_y, f_{xy} related to the x, y axes, and f_ξ, f_η, $f_{\xi\eta}$ related to the ξ, η axes. Those with a single subscript are direct stresses acting in the direction of the axis indicated by the subscript. Those with two subscripts are shear stresses associated with the axes indicated by the subscripts. Similarly, the strains are e_x, e_y, e_{xy}, e_ξ, e_η, and $e_{\xi\eta}$.

The two sets of stresses are related to each other by the equations:

$$f_\xi = f_x \cos^2 \theta + f_y \sin^2 \theta - 2f_{xy} \sin \theta \cos \theta$$

$$f_\eta = f_x \sin^2 \theta + f_y \cos^2 \theta + 2f_{xy} \sin \theta \cos \theta \tag{1}$$

$$f_{\xi\eta} = f_x \sin \theta \cos \theta - f_y \sin \theta \cos \theta + f_{xy} (\cos^2 \theta - \sin^2 \theta)$$

or

$$f_x = f_\xi \cos^2 \theta + f_\eta \sin^2 \theta + 2f_{\xi\eta} \sin \theta \cos \theta$$

$$f_y = f_\xi \sin^2 \theta + f_\eta \cos^2 \theta - 2f_{xy} \sin \theta \cos \theta \tag{2}$$

$$f_{xy} = -f_\xi \sin \theta \cos \theta + f_\eta \sin \theta \cos \theta + f_{\xi\eta} (\cos^2 \theta - \sin^2 \theta)$$

The two sets of strains are related to each other by the equations:

$$e_\xi = e_x \cos^2 \theta + e_y \sin^2 \theta - e_{xy} \sin \theta \cos \theta$$

$$e_\eta = e_x \sin^2 \theta + e_y \cos^2 \theta + e_{xy} \sin \theta \cos \theta \tag{3}$$

$$e_{\xi\eta} = 2e_x \sin \theta \cos \theta - 2e_y \sin \theta \cos \theta + e_{xy} (\cos^2 \theta - \sin^2 \theta)$$

or

$$e_x = e_\xi \cos^2\theta + e_\eta \sin^2\theta + e_{\xi\eta} \sin\theta \cos\theta$$

$$e_y = e_\xi \sin^2\theta + e_\eta \cos^2\theta - e_{\xi\eta} \sin\theta \cos\theta \tag{4}$$

$$e_{xy} = -2e_\xi \sin\theta\cos\theta + 2e_\eta \sin\theta\cos\theta + e_{\xi\eta}(\cos^2\theta - \sin^2\theta)$$

Equations (1), (2), (3), and (4) are arrived at by geometrical considerations. Therefore, they are independent of the properties of the material to which they are applied. Their derivations may be found in most any standard text on the theory of elasticity.

2. The relations Between Stress and Strain

According to the generalized Hooks' law, each strain is linearly related to the three stresses, which results in 9 elastic properties for each material. These 9 properties are not independent of each other because of the existence of a strain-energy function. The most general relation between strain and stress, in two dimensions, is given by:

$$e_\xi = r_{11} f_\xi + r_{12} f_\eta + r_{13} f_{\xi\eta}$$

$$e_\eta = r_{12} f_\xi + r_{22} f_\eta + r_{23} f_{\xi\eta} \tag{5}$$

$$e_{\xi\eta} = r_{13} f_\xi + r_{23} f_\eta + r_{33} f_{\xi\eta}$$

The inverse of this group of equations is:

$$f_\xi = s_{11} e_\xi + s_{12} e_\eta + s_{13} e_{\xi\eta}$$

$$f_\eta = s_{12} e_\xi + s_{22} e_\eta + s_{23} e_{\xi\eta} \qquad (6)$$

$$f_{\xi\eta} = s_{13} e_\xi + s_{23} e_\eta + s_{33} e_{\xi\eta}$$

These two sets of equations are related by:

$$r_{11} = \frac{s_{22} s_{33} - s_{23}^2}{S} \qquad r_{12} = \frac{s_{13} s_{23} - s_{12} s_{33}}{S}$$

$$r_{13} = \frac{s_{12} s_{23} - s_{13} s_{22}}{S} \qquad r_{22} = \frac{s_{11} s_{33} - s_{13}^2}{S}$$

$$r_{23} = \frac{s_{13} s_{12} - s_{11} s_{23}}{S} \qquad r_{33} = \frac{s_{11} s_{22} - s_{12}^2}{S} \qquad (7)$$

$$S = s_{11} s_{22} s_{33} - s_{11} s_{23}^2 + 2s_{12} s_{23} s_{13} - s_{12}^2 s_{33} - s_{13}^2 s_{22}$$

The inverse of this group of equations is identical in form; that is:

$$s_{11} = \frac{r_{22} r_{33} - r_{23}^2}{R} \quad \text{, etc.}$$

$$(8)$$

$$R = r_{11} r_{22} r_{33} - r_{11} r_{23}^2 + 2r_{12} r_{23} r_{13} - r_{12}^2 r_{33} - r_{13}^2 r_{22}$$

The meanings of some of the coefficients in equations (5) are made evident by letting two of the stresses be zero; thus:

$$r_{11} = \frac{1}{E_\xi} \qquad r_{12} = -\frac{\mu_{\xi\eta}}{E_\xi} = -\frac{\mu_{\eta\xi}}{E_\eta} \qquad r_{22} = \frac{1}{E_\eta} \qquad r_{33} = \frac{1}{G_{\xi\eta}}$$

Where E_ξ and E_η are the moduli of elasticity in the ξ and η directions, $G_{\xi\eta}$ is the modulus of rigidity associated with the ξ and η axes and $\mu_{\xi\eta}$ and $\mu_{\eta\xi}$ are Poisson's ratios of a contraction in the direction of the second subscript to an elongation in the direction of the first subscript due to a tensile stress in this last direction. The values of r_{13} and and r_{23} have to do with strain ratios involving shear strains.

3. Transformation of the Stress-Strain Equations

Equations (5) may be transformed to refer to the x, y axes by use of equations (1) and (4). The transformed equations are:

$$\begin{aligned} e_x &= a_{11} f_x + a_{12} f_y + a_{13} f_{xy} \\ e_y &= a_{12} f_x + a_{22} f_y + a_{23} f_{xy} \\ e_{xy} &= a_{13} f_x + a_{23} f_y + a_{33} f_{xy} \end{aligned} \tag{9}$$

Which are related to equations (5) by:

$$a_{11} = r_{11} \cos^4 \theta + 2r_{13} \cos^3 \theta \sin \theta + (2r_{12} + r_{33}) \cos^2 \theta \sin^2 \theta + 2r_{23} \cos \theta \sin^3 \theta + r_{22} \sin^4 \theta$$

$$a_{12} = r_{12} \cos^4 \theta + (r_{23} - r_{13}) \cos^3 \theta \sin \theta + (r_{11} + r_{22} - r_{33}) \cos^2 \theta \sin^2 \theta$$

$$+ (r_{13} - r_{23}) \cos \theta \sin^3 \theta + r_{12} \sin^4 \theta$$

(10)

$$a_{13} = r_{13} \cos^4 \theta + (2r_{12} + r_{33} - 2r_{11}) \cos^3 \theta \sin \theta + 3(r_{23} - r_{13}) \cos^2 \theta \sin^2 \theta$$

$$- (2r_{12} + r_{33} - 2r_{22}) \cos \theta \sin^3 \theta - r_{23} \sin^4 \theta$$

$$a_{22} = r_{22} \cos^4 \theta - 2r_{23} \cos^3 \theta \sin \theta + (2r_{12} + r_{33}) \cos^2 \theta \sin^2 \theta - 2r_{13} \cos \theta \sin^3 \theta + r_{11} \sin^4 \theta$$

 (Formulas (10) continued on next sheet)

(Formulas (10) continued)

$$a_{23} = r_{23} \cos^4\theta + (2r_{22} - 2r_{12} - r_{33}) \cos^3\theta \sin\theta + 3(r_{13} - r_{23}) \cos^2\theta \sin^2\theta$$

$$- (2r_{11} - 2r_{12} - r_{33}) \cos\theta \sin^3\theta - r_{13} \sin^4\theta$$

(10)

$$a_{33} = r_{33} \cos^4\theta + 4(r_{23} - r_{13}) \cos^3\theta \sin\theta + 2(2r_{22} + 2r_{11} - 4r_{12} - r_{33}) \cos^2\theta \sin^2\theta$$

$$+ 4(r_{13} - r_{23}) \cos\theta \sin^3\theta + a_{33} \sin^4\theta$$

in which $\underline{\theta}$ is measured positively counterclockwise from the $\underline{\xi}$ axis to the $\underline{x}$ axis.

These relations are obtained by letting the stresses associated with the x, y axes be zero except one; then, substituting this one stress in equations (1), values of f_ξ, f_η, and $f_{\xi\eta}$ are obtained. These values are substituted in equations (5) to obtain the related strains. These strains are then substituted in equations (4) (one equation at a time) so that the ratios of the strains to the stresses associated with the x, y axes are obtained, and the values of a are obtained by reference to equations (9).

Equations (6) may be transformed in a similar manner by using equations (1) and (4). The transformed equations are:

$$
\begin{aligned}
f_x &= b_{11} e_x + b_{12} e_y + b_{13} e_{xy} \\
f_y &= b_{12} e_x + b_{22} e_y + b_{23} e_{xy} \\
f_{xy} &= b_{13} e_x + b_{23} e_y + b_{33} e_{xy}
\end{aligned}
\tag{11}
$$

Which are related to equations (6) by:

$$b_{11} = s_{11} \cos^4\theta + 4s_{13}\cos^3\theta\sin\theta + 2(s_{12} + 2s_{33})\cos^2\theta\sin^2\theta + 4s_{23}\cos\theta\sin^3\theta + s_{22}\sin^4\theta$$

$$\begin{aligned} b_{12} = s_{12}\cos^4\theta + 2(s_{23} - s_{13})\cos^3\theta\sin\theta + (s_{11} + s_{22} - 4s_{33})\cos^2\theta\sin^2\theta \\ + 2(s_{13} - s_{23})\cos\theta\sin^3\theta + s_{12}\sin^4\theta \end{aligned} \tag{12}$$

$$\begin{aligned} b_{13} = s_{13}\cos^4\theta + (2s_{33} + s_{12} - s_{11})\cos^3\theta\sin\theta + 3(s_{23} - s_{13})\cos^2\theta\sin^2\theta \\ - (2s_{33} + s_{12} - s_{22})\cos\theta\sin^3\theta - s_{23}\sin^4\theta \end{aligned}$$

$$b_{22} = s_{22}\cos^4\theta - 4s_{23}\cos^3\theta\sin\theta + 2(2s_{33} + s_{12})\cos^2\theta\sin^2\theta - 4s_{13}\cos\theta\sin^3\theta + s_{11}\sin^4\theta$$

(Formulas (12) continued on next sheet)

(Formulas (12) continued)

$$b_{23} = s_{23} \cos^4 \theta - (2s_{33} + s_{12} - s_{22}) \cos^3 \theta \sin \theta + 3(s_{13} - s_{23}) \cos^2 \theta \sin^2 \theta$$

$$+ (2s_{33} + s_{12} - s_{11}) \cos \theta \sin^3 \theta - s_{13} \sin^4 \theta \qquad (12)$$

$$b_{33} = s_{33} \cos^4 \theta + 2(s_{23} - s_{13}) \cos^3 \theta \sin \theta + (s_{22} + s_{11} - 2s_{12} - 2s_{33}) \cos^2 \theta \sin^2 \theta$$

$$+ 2(s_{13} - s_{23}) \cos \theta \sin^3 \theta + s_{33} \sin^4 \theta$$

in which $\underline{\theta}$ is measured positively counterclockwise from the $\underline{\xi}$ axis to the $\underline{x}$ axis.

These relations are obtained by letting the strains associated with the $\underline{x}$, $\underline{y}$ axes be zero except one, then substituting this one strain in equations (3), and so on.

4. Orthotropic Materials

All of the equations given up to this point are perfectly general, and apply to all materials. They indicate that the most general material has radial symmetry. If various additional symmetries are imposed, the coefficients of equations (5) assume particular values. If a material has an axis of symmetry (α) it also has another axis of symmetry (β) at right angles to α, because of the radial symmetry, and the material is called orthotropic. It can be shown that, if equations (5) for such a material are written for the α and β axes, rather than for the arbitrary ξ and η axes, the values of r_{13} and r_{23} are zero and equations (5) become:

$$
\begin{aligned}
e_\alpha &= \frac{1}{E_\alpha} f_\alpha - \frac{\mu_{\alpha\beta}}{E_\alpha} f_\beta \\
e_\beta &= -\frac{\mu_{\beta\alpha}}{E_\beta} f_\alpha + \frac{1}{E_\beta} f_\beta \\
e_{\alpha\beta} &= \frac{1}{G_{\alpha\beta}} f_{\alpha\beta}
\end{aligned}
\tag{13}
$$

These equations may be transformed to refer to axes $\underline{x}$ and $\underline{y}$, making angles ϕ (measured positively counterclockwise from the α axis to the $\underline{x}$ axis as shown in figure 23) with the α and β axes by use of equations (9), so that:

$$
\begin{aligned}
e_x &= a_{11} f_x + a_{12} f_y + a_{13} f_{xy} \\
e_y &= a_{12} f_x + a_{22} f_y + a_{23} f_{xy} \\
e_{xy} &= a_{13} f_x + a_{23} f_y + a_{33} f_{xy}
\end{aligned}
\tag{14}
$$

Relations (10) become:

$$
\begin{aligned}
a_{11} &= \frac{\sin^4\phi}{E_\beta} + \frac{\cos^4\phi}{E_\alpha} + \left[\frac{1}{G_{\alpha\beta}} - \frac{2\mu_{\alpha\beta}}{E_\alpha}\right]\sin^2\phi\cos^2\phi \\
a_{12} &= \left[\frac{1}{E_\alpha} + \frac{1}{E_\beta} - \frac{1}{G_{\alpha\beta}}\right]\sin^2\phi\cos^2\phi - \frac{\mu_{\alpha\beta}}{E_\alpha}\left[\sin^4\phi + \cos^4\phi\right] \\
a_{13} &= \left[\frac{1}{G_{\alpha\beta}} - \frac{2\mu_{\alpha\beta}}{E_\alpha} - \frac{2}{E_\alpha}\right]\sin\phi\cos^3\phi - \left[\frac{1}{G_{\alpha\beta}} - \frac{2\mu_{\alpha\beta}}{E_\alpha} - \frac{2}{E_\beta}\right]\sin^3\phi\cos\phi \\
a_{22} &= \frac{\sin^4\phi}{E_\alpha} + \frac{\cos^4\phi}{E_\beta} + \left[\frac{1}{G_{\alpha\beta}} - \frac{2\mu_{\alpha\beta}}{E_\alpha}\right]\sin^2\phi\cos^2\phi \\
a_{23} &= \left[\frac{1}{G_{\alpha\beta}} - \frac{2\mu_{\alpha\beta}}{E_\alpha} - \frac{2}{E_\alpha}\right]\sin^3\phi\cos\phi - \left[\frac{1}{G_{\alpha\beta}} - \frac{2\mu_{\alpha\beta}}{E_\alpha} - \frac{2}{E_\beta}\right]\sin\phi\cos^3\phi \\
a_{33} &= 4\left[\frac{1}{E_\alpha} + \frac{1}{E_\beta} + \frac{2\mu_{\alpha\beta}}{E_\alpha}\right]\sin^2\phi\cos^2\phi + \frac{1}{G_{\alpha\beta}}\left[\cos^2\phi - \sin^2\phi\right]^2
\end{aligned}
\tag{15}
$$

The inverse of this group of equations (13) is obtained by using equations (6) and relations (8). They are:

$$f_\alpha = \frac{E_\alpha}{\lambda} e_\alpha + \frac{E_\alpha \mu_{\beta\alpha}}{\lambda} e_\beta$$

$$f_\beta = \frac{E_\beta \mu_{\alpha\beta}}{\lambda} e_\alpha + \frac{E_\beta}{\lambda} e_\beta$$

$$f_{\alpha\beta} = G_{\alpha\beta} e_{\alpha\beta} \tag{16}$$

$$\lambda = 1 - \mu_{\alpha\beta} \mu_{\beta\alpha}$$

These equations may be transformed to refer to axes x and y by use of equations (11). The transformed equations are:

$$f_x = b_{11} e_x + b_{12} e_y + b_{13} e_{xy}$$

$$f_y = b_{12} e_x + b_{22} e_y + b_{23} e_{xy} \tag{17}$$

$$f_{xy} = b_{13} e_x + b_{23} e_y + b_{33} e_{xy}$$

Relations (12) become:

$$
\begin{aligned}
b_{11} &= \frac{1}{\lambda}\left[E_\alpha \cos^4 \phi + E_\beta \sin^4 \phi + (2E_\alpha \mu_{\beta\alpha} + 4\lambda G_{\alpha\beta}) \sin^2 \phi \cos^2 \phi\right] \\
b_{12} &= \frac{1}{\lambda}\left[(E_\alpha + E_\beta - 4\lambda G_{\alpha\beta}) \sin^2 \phi \cos^2 \phi + E_\alpha \mu_{\beta\alpha} (\cos^4 \phi + \sin^4 \phi)\right] \\
b_{13} &= \frac{1}{\lambda}\left[(E_\beta - E_\alpha \mu_{\beta\alpha} - 2\lambda G_{\alpha\beta}) \sin^3 \phi \cos \phi - (E_\alpha - E_\alpha \mu_{\beta\alpha} - 2\lambda G_{\alpha\beta}) \sin \phi \cos^3 \phi\right] \\
b_{22} &= \frac{1}{\lambda}\left[E_\beta \cos^4 \phi + E_\alpha \sin^4 \phi + (2E_\alpha \mu_{\beta\alpha} + 4\lambda G_{\alpha\beta}) \sin^2 \phi \cos^2 \phi\right] \\
b_{23} &= \frac{1}{\lambda}\left[(E_\beta - E_\alpha \mu_{\beta\alpha} - 2\lambda G_{\alpha\beta}) \sin \phi \cos^3 \phi - (E_\alpha - E_\alpha \mu_{\beta\alpha} - 2\lambda G_{\alpha\beta}) \sin^3 \phi \cos \phi\right] \\
b_{33} &= \frac{1}{\lambda}\left[(E_\alpha + E_\beta - 2E_\alpha \mu_{\beta\alpha}) \sin^2 \phi \cos^2 \phi + \lambda G_{\alpha\beta} (\cos^2 \phi - \sin^2 \phi)^2\right]
\end{aligned}
\tag{18}
$$

where ϕ is measured positively counterclockwise from the α axis to the x axis.

5. Laminates

Consider a laminate made up of n individual laminations. The properties of each lamination associated with certain orthogonal axes ξ_i and η_i are assumed to be known. The individual laminations are orientated in the laminate so that the axes ξ_i make angles ψ_i with an arbitrarily chosen ξ axis with the values of ψ_i measured positively counterclockwise from the ξ_i axis to the ξ axis, as shown in figure 23. Equations (5) and (6) hold for each lamination, and it is assumed that a sufficient number of the r's and s's are known for each lamination so that they are all known because of relations (7) and (8). Equations (11) can then be written for each lamination thus:

$$
\begin{aligned}
f_{\xi i} &= b_{11i}\, e_{\xi} + b_{12i}\, e_{\eta} + b_{13i}\, e_{\xi\eta} \\
f_{\eta i} &= b_{12i}\, e_{\xi} + b_{22i}\, e_{\eta} + b_{23i}\, e_{\xi\eta} \\
f_{\xi\eta i} &= b_{13i}\, e_{\xi} + b_{23i}\, e_{\eta} + b_{33i}\, e_{\xi\eta}
\end{aligned}
\qquad (19)
$$

The values of the coefficients to each lamination are given by relations (12) by replacing θ by ψ_i. The stresses $f_{\xi i}$, $f_{\eta i}$, and $f_{\xi\eta i}$ are those associated with the ξ, η axes in the ith lamination.

Because the laminations are cemented together in the unstrained condition, the strains in equation (19) apply to all the laminations and to the laminate. The values of the stresses in the individual laminations vary from lamination to lamination according to equations (19). The average stresses in the laminate are given by:

$$
f_{\xi} = \frac{1}{t} \sum_{i=1}^{i=n} t_i f_{\xi i} \qquad f_{\eta} = \frac{1}{t} \sum_{i=1}^{i=n} t_i f_{\eta i} \qquad f_{\xi\eta} = \frac{1}{t} \sum_{i=1}^{i=n} t_i f_{\xi\eta i} \qquad (20)
$$

in which t is the thickness of the laminate and t_i is the thickness of an individual lamination.

Substituting equations (19) into equations (20):

$$
\begin{aligned}
f_\xi &= \frac{e_\xi}{t}\sum t_i b_{11i} + \frac{e_\eta}{t}\sum t_i b_{12i} + \frac{e_{\xi\eta}}{t}\sum t_i b_{13i} \\
f_\eta &= \frac{e_\xi}{t}\sum t_i b_{12i} + \frac{e_\eta}{t}\sum t_i b_{22i} + \frac{e_{\xi\eta}}{t}\sum t_i b_{23i} \qquad (21) \\
f_{\xi\eta} &= \frac{e_\xi}{t}\sum t_i b_{13i} + \frac{e_\eta}{t}\sum t_i b_{23i} + \frac{e_{\xi\eta}}{t}\sum t_i b_{33i}
\end{aligned}
$$

These equations are identical to equations (6) with:

$$
\begin{aligned}
s_{11} &= \frac{1}{t}\sum t_i b_{11i} \qquad s_{12} = \frac{1}{t}\sum t_i b_{12i} \qquad s_{13} = \frac{1}{t}\sum t_i b_{13i} \\
& \qquad\qquad\qquad\qquad\qquad\qquad\qquad\qquad (22) \\
s_{22} &= \frac{1}{t}\sum t_i b_{22i} \qquad s_{23} = \frac{1}{t}\sum t_i b_{23i} \qquad s_{33} = \frac{1}{t}\sum t_i b_{33i}
\end{aligned}
$$

They can be put in the form of equations (5) by use of the relations (7). These equations can then be transformed to any arbitrarily chosen $\underline{x}$, $\underline{y}$ axes, the $\underline{x}$ axis making an angle $\underline{\theta}$ with the $\underline{\xi}$ axis (as shown in figure 23) according to equations (9) and relations (10). Thus the properties of the laminate are known in any direction.

If the individual laminations are orthotropic, it is convenient to choose $\underline{\xi_i}$ and $\underline{\eta_i}$ parallel to the natural axes $\underline{\alpha_i}$ and $\underline{\beta_i}$. The coefficients of equations (19) are then given by relations (18) rather than the more general relations (12).

6. Strength of Laminates Made of Orthotropic Laminations

It is assumed that the elastic properties of the laminate associated with the ξ, η axes have been computed (that is, values of r for use in equations (5) are known).

The laminate is subjected to the stresses f_x, f_y, and f_{xy} (associated with the x, y axes) which are held proportional to each other until failure takes place. The angle θ is measured positively counterclockwise from the ξ axis to the x axis (fig. 24). The strains associated with these stresses are obtained from equations (9), using the values of r, previously obtained, in equations (10) to obtain values of a. These strains are transformed to the ξ_i, η_i axes, the natural axes of the individual laminations, by means of equations (3) (fig. 24), thus:

$$
\begin{aligned}
e_{\alpha i} &= e_x \cos^2(\psi_i + \theta) + e_y \sin^2(\psi_i + \theta) - e_{xy} \sin(\psi_i + \theta)\cos(\psi_i + \theta) \\
e_{\beta i} &= e_x \sin^2(\psi_i + \theta) + e_y \cos^2(\psi_i + \theta) + e_{xy} \sin(\psi_i + \theta)\cos(\psi_i + \theta) \\
e_{\alpha\beta i} &= 2e_x \sin(\psi_i + \theta)\cos(\psi_i + \theta) - 2e_y \sin(\psi_i + \theta)\cos(\psi_i + \theta) \\
&\quad + e_{xy}\left[\cos^2(\psi_i + \theta) - \sin^2(\psi_i + \theta)\right]
\end{aligned}
\tag{24}
$$

The stresses to which the individual lamination is subjected are found from these strains by means of equations (16), thus:

$$
\begin{aligned}
f_{\alpha i} &= \frac{E_{\alpha i}}{\lambda_i} e_{\alpha i} + \frac{E_{\alpha i}\mu_{\beta\alpha i}}{\lambda_i} e_{\beta i} \\
f_{\beta i} &= \frac{E_{\beta i}\mu_{\alpha\beta i}}{\lambda_i} e_{\alpha i} + \frac{E_{\beta i}}{\lambda_i} e_{\beta i} \\
f_{\alpha\beta i} &= G_{\alpha\beta i}\, e_{\alpha\beta i}
\end{aligned}
\tag{25}
$$

Each individual lamination will fail when:[4,5,6]

$$\frac{f_{\alpha i}^2}{F_{\alpha i}^2} - \frac{f_{\alpha i}\, f_{\beta i}}{F_{\alpha i}\, F_{\beta i}} + \frac{f_{\beta i}^2}{F_{\beta i}^2} + \frac{f_{\alpha\beta i}^2}{F_{\alpha\beta i}^2} = 1 \tag{26}$$

In which $F_{\alpha i}$, $F_{\beta i}$, and $F_{\alpha\beta i}$ are the strengths of the individual laminations associated with the stresses $f_{\alpha i}$, $f_{\beta i}$, and $f_{\alpha\beta i}$, each acting alone. Each of the strengths $F_{\alpha i}$ and $F_{\beta i}$ have two values, one in tension and one in compression. If the associated stress is negative, the compressive strength is used; if positive, the tensile strength is used. The strengths have the same signs as the stresses, so that the ratios are always positive.

Thus, values of f_x, f_y, or f_{xy} are obtained at which the individual laminations will fail, one value for each lamination. The value of this stress at which the laminate, as a whole, will fail is at least as great as the least of its values associated with failure of the individual laminations, and will lie between this least value and the average of the values associated with the individual laminations.

7. A Laminate Made of Two Identical Orthotropic Laminations

Consider a laminate made of two identical orthotropic laminations placed so that the angle between their natural axes α_1 and α_2 is 2ϕ. Choose the direction of the ξ axis so that it bisects this angle, thus $\phi_1 = \phi$ and $\phi_2 = -\phi$ (fig. 25). In making the summations indicated by equations (22),

[4]Norris, C. B., and McKinnon, P. F. Compression, Tension, and Shear Tests on Yellowpoplar Plywood Panels of Sizes That Do Not Buckle With Tests Made at Various Angles to the Face Grain. Forest Products Laboratory Report No. 1328. 42 pp., Illus. 1946.

[5]Werren, Fred, and Norris, C. B. Directional Properties of Glass-Fabric-Base Plastic Laminate Panels of Sizes That Do Not Buckle. Forest Products Laboratory Report No. 1803. 49 pp., Illus. 1949.

[6]Norris, Charles B. Strength of Orthotropic Materials Subjected to Combined Stresses. Forest Products Laboratory Report No. 1816. 34 pp., Illus. 1955.

it will be noticed that in relations (18) a change in sign of ϕ changes the sign of b_{13} and b_{23} and does not change the sign of the other coefficients. Thus

$$s_{11} = b_{11i} \qquad s_{12} = b_{12i} \qquad s_{13} = 0$$
$$s_{22} = b_{22i} \qquad s_{23} = 0 \qquad s_{33} = b_{33i} \tag{27}$$

Equations (6) become

$$f_{\xi} = b_{11i}\, e_{\xi} + b_{12i}\, e_{\eta}$$
$$f_{\eta} = b_{12i}\, e_{\xi} + b_{22i}\, e_{\eta} \tag{28}$$
$$f_{\xi\eta} = b_{33i}\, e_{\xi\eta}$$

These equations show that the laminate is orthotropic and that the ξ and η axes are its natural axes. By comparison of equations (28) with equations (16):

$$b_{11i} = \frac{E_{\xi}}{\lambda} \qquad b_{12i} = \frac{E_{\xi}\, \mu_{\eta\xi}}{\lambda} \qquad b_{22i} = \frac{E_{\eta}}{\lambda} \qquad b_{33i} = G_{\xi\eta} \tag{29}$$

Solving these equations for the elastic properties, or using relations (7):

$$E_{\xi} = b_{11i} - \frac{b_{12i}^2}{b_{22i}} \qquad E_{\eta} = b_{22i} - \frac{b_{12i}^2}{b_{11i}}$$
$$\mu_{\eta\xi} = \frac{b_{12i}}{b_{11i}} \qquad \lambda = 1 - \frac{b_{12i}^2}{b_{11i}\, b_{22i}} \tag{30}$$

8. A Laminate Made of a Number of Different Orthotropic Laminations Either Cross or Parallel Laminated

A laminate is made of a number of orthotropic laminations placed with their natural axes (α_i) parallel to each other. The natural axis $(\underline{\alpha})$ of the laminate is parallel to those of the individual laminations. Equations (22) become:

$$s_{11} = \frac{1}{t}\sum t_i \frac{E_{\alpha i}}{\lambda_i} \qquad s_{12} = \frac{1}{t}\sum t_i \frac{E_{\alpha i}\,\mu_{\beta\alpha i}}{\lambda} \qquad s_{13} = 0$$

$$s_{22} = \frac{1}{t}\sum t_i \frac{E_{\beta i}}{\lambda_i} \qquad s_{23} = 0 \qquad s_{33} = \frac{1}{t}\sum t_i\, G_{\alpha\beta i} \tag{31}$$

Using relations (7):

$$E_\alpha = \frac{1}{t}\sum t_i \frac{E_{\alpha i}}{\lambda_i} - \frac{1}{t}\,\frac{\left(\sum t_i \frac{E_{\alpha i}\,\mu_{\beta\alpha i}}{\lambda_i}\right)^2}{\sum t_i \frac{E_{\beta i}}{\lambda_i}}$$

$$E_\beta = \frac{1}{t}\sum t_i \frac{E_{\beta i}}{\lambda_i} - \frac{1}{t}\,\frac{\left(\sum t_i \frac{E_{\alpha i}\,\mu_{\beta\alpha i}}{\lambda_i}\right)^2}{\sum t_i \frac{E_{\alpha i}}{\lambda_i}} \tag{32}$$

$$\mu_{\beta\alpha} = \frac{\sum t_i \frac{E_{\alpha i}\,\mu_{\beta\alpha i}}{\lambda_i}}{\sum t_i \frac{E_{\alpha i}}{\lambda_i}} \qquad \mu_{\alpha\beta} = \frac{\sum t_i \frac{E_{\alpha i}\,\mu_{\beta\alpha i}}{\lambda_i}}{\sum t_i \frac{E_{\beta i}}{\lambda_i}}$$

$$G_{\alpha\beta} = \frac{1}{t}\sum t_i\, G_{\alpha\beta i}$$

Table 1.--Assembly data and some physical properties of the glass-fabric laminates. Resin 2[1] was used.

Panel No.	Fabric	Orientation of warp direction	Total number of laminations	Curing pressure	Resin content of panel	Average thickness of panel	Specific gravity	Barcol hardness
				P.s.i.	Percent	Inch		
1	143-114	Parallel	12	8	34.6	0.121	1.80	61
2	181-114	....do.....	12	30	36.1	.125	1.79	65
3	162-114	....do.....	8	30	36.9	.117	1.76	61
4	143-114	....(2)....	12	9	36.6	.128	1.76	62
5	143-114	....(3)....	13	10	36.9	.137	1.79	61
6	Composite[4]	....(3)....	12	30	34.8	.133	1.80	61

[1] Resin 2 is a high-temperature-setting, low-viscosity, laminating resin of the polyester (styrene-alkyd) type.

[2] Illustrated in figure 2.

[3] Illustrated in figure 3.

[4] Panel 6 consisted of 4 laminations of 143-114, 3 laminations of 162-114, and 5 laminations of 181-114 fabric.

Table 2.--Results of tension tests of glass-fabric parallel-laminated panels 1, 2, and 3.[1]

Panel No.	Glass fabric	Direction of test and modulus		Elastic moduli (1,000 p.s.i.): Modulus of elasticity, initial loading phase: Initial[2]	Secondary[3]	Unloading phase	Elastic moduli, reloading phase: Initial[2]	Secondary[3]	Direction of test and stress	Stress (P.s.i.): Proportional limit stress, initial loading phase: Initial	Secondary	Stress before unloading	Proportional limit stress, reloading phase: Initial	Secondary	Ultimate stress
1	143-114	E_0	max.	4,525	4,266	4,595	4,598	4,395	F_0	58,530	...	61,480	46,330	75,820	85,550
			min.	4,274	3,167	4,348	4,276	3,782		30,910	...	50,060	41,220	62,080	69,960
			av.	4,366	3,780[4]	4,493[4]	4,441[5]	4,012[5]		46,700	61,280[1]	53,930[4]	44,730[5]	68,320[4]	79,490
		E_{90}	max.	1,539	419	1,055	962	742	F_{90}	3,270	7,520	8,130	4,360	8,040	9,930
			min.	1,173	397	677	744	370		2,410	6,550	4,290	1,520	4,570	9,450
			av.	1,350	409	783[5]	875[5]	601[5]		2,840	7,090[4]	6,860[5]	2,660[5]	6,050[5]	9,670
		E_{45}	max.	1,465	...	...	...	...	F_{45}	4,620	...	...	...	...	13,220
			min.	932	...	...	...	...		3,540	...	...	...	...	12,450
			av.	1,330	...	...	...	...		4,100	...	...	...	...	12,850
		G_{0-90}[4]		472	2,044	634	585	...	...	...	...	...	...	...	...
2	181-114	E_0	max.	3,306	2,460	2,681	2,720	2,473	F_0	9,430	33,870	34,190	27,770	34,190	43,840
			min.	2,466	2,150	2,496	2,621	2,234		6,030	25,160	26,520	13,760	26,520	37,950
			av.	2,921	2,316	2,620[4]	2,658[5]	2,387[4]		7,740	29,490[4]	30,300[5]	20,830[5]	29,500[4]	41,720
		E_{90}	max.	3,082	2,471	2,721	2,721	2,503	F_{90}	8,490	34,450	32,540	25,890	41,380	48,380
			min.	2,791	2,316	2,642	2,553	2,270		6,100	25,760	26,110	12,880	30,870	44,410
			av.	2,948	2,386	2,689[5]	2,644[5]	2,373[5]		7,600	29,330[4]	29,620[5]	22,140[5]	33,320[5]	46,380
		E_{45}	max.	1,720	...	...	...	...	F_{45}	4,960	...	...	...	...	21,440
			min.	1,460	...	...	...	...		3,410	...	...	...	...	19,460
			av.	1,569	...	...	...	...		4,260	...	...	...	...	20,640
		G_{0-90}[4]		516	575	540	539	...	...	...	...	...	...	...	...
3	162-114	E_0	max.	2,928	2,494	2,837	2,837	2,450	F_0	14,420	26,620	25,610	24,960	25,610	48,900
			min.	2,736	2,218	2,668	2,584	2,411		7,550	21,340	21,190	11,860	23,720	45,790
			av.	2,824	2,386	2,772[5]	2,729[5]	2,430[2]		10,000	23,930[3]	22,950[5]	19,090[5]	24,660[2]	46,900
		E_{90}	max.	2,179	1,651	1,983	1,962	1,660	F_{90}	6,460	12,530	13,990	11,070	15,290	32,150
			min.	1,886	1,538	1,818	1,734	1,387		4,360	10,180	9,680	9,640	13,390	27,410
			av.	2,039	1,575	1,895[5]	1,870[5]	1,531[5]		5,730	11,610[3]	12,000[5]	10,390[5]	14,780[5]	29,620
		E_{45}	max.	1,606	...	...	...	...	F_{45}	4,860	...	...	...	...	18,060
			min.	1,332	...	...	...	...		3,220	...	...	...	...	16,700
			av.	1,446	...	...	...	...		4,150	...	...	...	...	17,480
		G_{0-90}[4]		496	551	507	510	...	...	...	...	...	...	...	...

[1]Each average value represents the average of six tests, except where footnote-type number used with an average value indicates the number of tests represented in the value given.

[2]Based on initial straight-line portion (lower slope) of load-deformation curve.

[3]Based on second straight-line portion (upper slope) of load-deformation curve.

[4]Calculated values of $G_{\alpha\beta}$ from $\frac{1}{G_{\alpha\beta}} = \frac{4}{E_{45}} - \frac{1}{E_{90}} (1 - \mu_{\beta\alpha}) - \frac{1}{E_0} (1 - \mu_{\alpha\beta})$, using data from this table and table 4.

Table 3.--Results of compression tests of parallel-laminated glass-fabric panels 1, 2, and 3.

Panel No.	Fabric	Stress direction[1] and specimen number	Modulus of elasticity	Stress at -- Proportional limit	Stress at -- Ultimate
			1,000 p.s.i.	P.s.i.	P.s.i.
1	143-114	0° -- 1-1	4,559	33,740	54,460
		0° -- 1-2	4,506	30,100	53,460
		0° -- 1-3	4,570	33,130	54,840
		Average	4,545	32,320	54,250
		90° -- 1-1	1,477	9,850	22,340
		90° -- 1-2	1,612	8,940	22,040
		90° -- 1-3	1,610	9,020	21,970
		Average	1,566	9,270	22,120
2	181-114	0° -- 2-1	3,221	21,740	41,000
		0° -- 2-2	3,213	24,900	43,420
		0° -- 2-3	3,211	23,760	40,240
		Average	3,215	23,470	41,550
		90° -- 2-1	3,104	14,900	34,120
		90° -- 2-2	3,141	13,980	34,170
		90° -- 2-3	3,030	17,120	33,460
		Average	3,092	15,330	33,920
3	162-114	0° -- 3-1	3,021	13,530	21,650
		0° -- 3-2	3,031	13,910	19,640
		0° -- 3-3	2,946	12,610	20,180
		Average	2,999	13,350	20,490
		90° -- 3-1	2,225	12,790	23,030
		90° -- 3-2	2,228	13,590	21,330
		90° -- 3-3	2,192	13,480	16,010
		Average	2,215	13,290	20,120

[1] Direction of applied stress with respect to the warp direction of the laminations.

Table 4.--Poisson's ratios of parallel-laminated glass-fabric panels 1, 2, and 3.

Panel No.	Fabric	Direction of stress	Specimen No.	Ratios of contractions to extensions: First loading run: Initial[1]	First loading run: Secondary[2]	Unloading, first run, Initial[1]	Second loading run: Initial[1]	Second loading run: Secondary[2]	Fourth loading run: Initial[1]	Fourth loading run: Secondary[2]
1	143-114	0°	1-2	0.222	....	0.213	0.210	....	0.221	....
		0°	1-5	.217	....	.212	.212	....	.212	....
		0°	1-8	.218	....	.218	.221	....	.218	....
		$\mu_{\alpha\beta}$ average		.219	....	.214	.214	....	.217	....
		90°	1-2	.068	....	.032	.032	....	.033	0.024
		90°	1-5	.055	....	.026	.033	....	.031	.023
		90°	1-8	.059	....	.023	.032	0.021	.027	.020
		$\mu_{\beta\alpha}$ average		.060	....	.027	.032	.021	.030	.022
2	181-114	0°	2-2	.098	0.046	.080	.082	.074	.078	....
		0°	2-5	.116	.057	.081	.094	.078	.081	....
		0°	2-8	.107	.049	.073	.085	.063	.073	....
		$\mu_{\alpha\beta}$ average		.107	.051	.078	.087	.072	.077	....
		90°	2-2	.110	.055	.074	.076	....	.072	....
		90°	2-5	.093	.039	.070	.067	....	.065	....
		90°	2-8	.087	.046	.066	.062	....	.066	....
		$\mu_{\beta\alpha}$ average		.097	.047	.070	.068	....	.068	....
3	162-114	0°	3-2	.138	.145	.132	.135	....	.133	....
		0°	3-5	.132	.114	.119	.129	....	.127	....
		0°	3-8	.139	.123	.134	.140	....	.134	....
		$\mu_{\alpha\beta}$ average		.136	.127	.128	.134	....	.131	....
		90°	3-2	.091	.072	.082	.079	....	.079	....
		90°	3-5	.107	.084	.111	.096	....	.089	....
		90°	3-8	.092	.073	.079	.083	....	.078	....
		$\mu_{\beta\alpha}$ average		.097	.076	.091	.086	....	.082	....

[1] Based on ratios of initial straight-line portions (lower slopes) of load-deformation curves.

[2] Based on ratios of second straight-line portions (upper slopes) of load-deformation curves.

Table 5.--Strength and stress-strain ratios for tensile specimens cut from panel 5 at various angles to an arbitrary axis of reference.[1]

Angle of loading	Specimen number	Ultimate stress	Ratios for 0° strains (1,000 p.s.i.)				Ratios for 90° strains (1,000 p.s.i.)				Ratios for 45° strains (1,000 p.s.i.)			
			Initial	Secondary	Unloading	Reloading	Initial	Secondary	Unloading	Reloading	Initial	Secondary	Unloading	Reloading
		P.s.i.												
0°	5-1	60,650	3,685	3,348			13,666	15,627			7,636	6,052		
	5-2	60,540	3,522	3,208	3,438	3,438	14,428	16,556	14,256	14,200	14,034	18,145	15,159	14,089
	5-3	62,010	3,484		3,604	3,604	13,159	14,751	14,751	14,517	16,045	20,552	18,760	15,975
	Average	61,070	3,564	3,363	3,521	3,521	13,751	15,645	14,504	14,359				
30°	5-1	18,700	2,367				6,740	5,276			3,238	1,173		
	5-2	17,880	1,892		1,224	1,469	6,736	4,711	5,089	6,263	3,070		1,446	2,058
	5-3	17,550	2,148		1,227	1,484	7,389	5,547	5,598	6,199				
	Average	18,040	2,136	2,136	1,226	1,477	6,955	5,178	5,344	6,231				
45°	5-1	14,090	1,836				6,351	4,031			3,300			
	5-2	13,750	1,594		819	1,030	5,523	3,540	2,526	3,066	4,075		1,541	1,871
	5-3	13,600	1,387		916	1,221	5,723	3,897	2,935	3,330	3,330		1,761	2,289
	Average	13,810	1,606	1,606	868	1,126	5,866	3,823	2,730	3,198				
60°	5-1	13,170	1,494				4,916				3,860			
	5-2	13,060	1,446		987	1,138	5,211		3,285	3,746	4,221		2,776	2,924
	5-3	12,340	2,142		1,982	1,961			6,295	7,031	7,829		5,354	4,982
	Average	12,860	1,694	1,694	1,484	1,549	5,064	5,064	4,790	5,388				
90°	5-1	15,640	1,996	793			9,760				2,922			
	5-2	15,880	1,794		1,447	1,495	11,140		1,114	1,107	3,450		2,254	2,458
	5-3	15,670	1,783		1,324	1,385	10,170		1,185	1,193	3,783		2,144	2,369
	Average	15,730	1,858	1,457	1,386	1,440	10,360	10,360	1,150	1,150				
120°	5-1	30,590	2,275	1,545			6,201				5,223			
	5-2	30,810	2,226	1,667	1,946	2,065	6,016		5,483	6,545	6,196		4,363	4,624
	5-3	29,680	3,377		4,331	4,045			18,405	17,697	11,223		11,576	10,763
	Average	30,360	2,626	2,176	3,139	3,055	6,108	6,108	11,944	12,121				
135°	5-1	31,940	2,261	1,698			4,646	3,480			5,896	4,437		
	5-2	32,270	2,169	1,668	2,044	2,130	5,200		3,323	5,542	6,826		6,118	6,139
	5-3	32,720	2,225	1,778	1,922	2,157	5,202	3,281	3,210	4,954	13,399		13,399	12,455
	Average	32,310	2,218	1,715	1,983	2,144	5,016	3,989	3,267	5,248				
150°	5-1	36,450	2,683	1,990			5,116	3,837			34,174			
	5-2	37,720	2,651	2,223	2,237	2,594	5,792	4,474	3,942	4,837	6,150	5,248	4,971	5,507
	5-3	36,740	2,613	2,090	2,417	2,713	5,570	4,191	4,191	5,769	98,713			
	Average	36,970	2,649	2,101	2,327	2,654	5,493	4,167	4,067	5,303				

[1] Average secondary values of E_0 (vertical) and E_{90} (horizontal) represent the average of the given secondary values and the initial values wherever secondary values are missing.

Table 6.--Strength and stress-strain ratios for tensile specimens cut from panel 6 at various angles to an arbitrary axis of reference.[1]

Angle of loading	Specimen number	Ultimate stress	Ratios for 0° strains (1,000 p.s.i.)				Ratios for 90° strains (1,000 p.s.i.)				Ratios for 45° strains (1,000 p.s.i.)			
			Initial	Secondary	Unloading	Reloading	Initial	Secondary	Unloading	Reloading	Initial	Secondary	Unloading	Reloading
		P.s.i.												
0°	6-1	45,960	2,778	2,431			7,634				10,408	12,235		
	6-2	45,590	2,900	2,707	2,935	2,995	8,014	6,090	6,767	7,054	10,748		13,738	11,942
	6-3	45,550	2,720		2,642	2,680	7,622	6,664	6,916	7,622	7,654	6,776	7,654	7,622
	Average	45,700	2,799	2,619	2,789	2,838	7,757	6,796	6,842	7,338				
30°	6-1	41,930	2,731	2,298			8,053	6,079			14,495			
	6-2	43,280	2,667		2,460	2,612	8,628	5,882	6,887	8,234	14,739		14,854	13,875
	6-3	41,210	2,443		2,443	2,561	7,671	6,690	7,471	6,953	14,447		15,867	13,854
	Average	42,140	2,614	2,469	2,452	2,587	8,117	6,217	7,179	7,594				
45°	6-1	32,220	2,368	1,801			7,702	6,436			5,198			
	6-2	31,790	2,780		3,094	2,997					7,861		7,463	6,614
	6-3	32,570	2,398		2,110	2,312	7,432	6,032	6,329	7,123	11,770		12,699	11,094
	Average	32,190	2,515	2,326	2,602	2,654	7,592	6,234	6,329	7,123				
60°	6-1	28,810	2,342	1,803			6,762	5,503			7,386			
	6-2	29,290	2,109	1,534	1,822	2,000	7,321	5,465	6,044	7,185	8,186		7,886	7,699
	6-3	29,960	2,187	1,613	1,848	2,082	6,809	5,623	5,623	7,053	4,697		3,992	4,152
	Average	29,350	2,213	1,650	1,835	2,041	6,964	5,530	5,834	7,119				
90°	6-1	24,440	2,278	1,618			7,687	6,029			4,566	3,448		
	6-2	24,130	1,880	1,251	1,546	1,648	7,249	5,421	7,166	7,481	4,723	3,253	3,880	4,156
	6-3	23,690	1,799		1,516	1,593	7,040		6,573	7,147	4,476		3,983	4,140
	Average	24,090	1,986	1,556	1,531	1,620	7,325	6,160	6,870	7,314				
120°	6-1	24,060	2,029	1,429			7,399	11,164			9,434			
	6-2	24,130	2,090	1,527	1,790	1,938	6,152	5,014	5,938	6,472	6,319	4,618	5,167	5,329
	6-3	23,550	1,854		1,570	1,727	7,566	5,856	6,636	6,804	7,418	4,978	5,563	5,580
	Average	23,910	1,991	1,603	1,680	1,833	7,039	7,345	6,287	6,638				
135°	6-1	26,920	2,090	1,557			7,425	6,368			7,692	7,070		
	6-2	26,350	2,492	1,897	2,444	2,368	11,413	9,530	10,032	8,664	12,498		18,778	11,913
	6-3	24,340	2,215	1,699	2,036	2,047	9,239	7,229	7,201	7,256	4,498	3,157	4,047	3,946
	Average	25,870	2,266	1,718	2,240	2,208	9,359	7,709	8,617	7,960				
150°	6-1	29,720	2,287	1,832			7,701	6,462			13,478	14,684		
	6-2	29,650	2,350	1,948	2,292	2,335	6,962	5,480	5,820	7,430	5,026	3,828	4,262	4,688
	6-3	29,550	2,462		2,512	2,546	11,992	8,851	8,046	8,936	11,130		12,228	11,690
	Average	29,640	2,366	2,080	2,402	2,440	8,885	6,931	6,933	8,183				

[1] Average secondary values of E_0 (vertical) and E_{90} (horizontal) represent the average of the given secondary values and the initial values wherever secondary values are missing.

Table 7.--Experimental and computed tensile properties of an orthotropic glass-fabric 143-114 laminate, panel 4.

Stress direction and specimen number	Elastic properties (1,000 p.s.i.): Modulus of elasticity, initial loading phase: Initial[1]	Modulus of elasticity, initial loading phase: Secondary[2]	Elastic moduli, unloading phase: Initial[1]	Elastic moduli, unloading phase: Secondary[2]	Elastic moduli, reloading phase: Initial[1]	Elastic moduli, reloading phase: Secondary[2]		Strength properties (P.s.i.): Proportional limit stress, initial loading phase: Initial	Proportional limit stress, initial loading phase: Secondary	Stress before unloading	Proportional limit stress, reloading phase: Initial	Proportional limit stress, reloading phase: Secondary		Ultimate stress
EXPERIMENTAL VALUES OBTAINED FROM TENSION TESTS														
0° -- 4-2	3,703	3,195	....	....	....	....		25,750	47,540	....	....	....	F_0	63,490
0° -- 4-4	3,502	3,184	3,534	3,796	3,666	3,441		23,530	43,150	47,070	23,530	47,070		67,270
0° -- 4-6	3,589	3,341	3,492	3,751	3,657	3,511		25,190	44,570	46,510	27,130	46,510		66,280
Av. E_0	3,598	3,240	3,513	3,774	3,662	3,476	Av.	24,820	45,090	46,790	25,330	46,790	Av.	65,680
90° -- 4-1	1,551	429	....	....	....	....		2,770	5,540	....	....	....	F_{90}	9,930
90° -- 4-3	1,293	412	607	795	786	622		2,760	6,260	7,010	3,510	6,510		10,020
90° -- 4-5	1,182	462	736	799	848	717		3,170	6,340	6,830	2,440	5,850		9,510
Av. E_{90}	1,342	434	672	797	817	670	Av.	2,900	6,050	6,920	2,980	6,180	Av.	9,820
45° -- 4-1	1,130	506	....	....	....	....		2,910	7,290	....	....	....	F_{45}	10,980
45° -- 4-2	1,560	....	1,313	1,663	1,331	....		3,990	....	7,980	4,990	....		16,970
45° -- 4-3	2,004	1,206	1,683	1,925	1,964	1,671		3,930	6,870	7,850	2,950	6,380		16,990
Av. E_{45}	1,565	856	1,498	1,794	1,648	1,671	Av.	3,610	7,080	7,920	3,970	6,380	Av.	14,980
COMPUTED ELASTIC PROPERTIES							COMPUTED ULTIMATE STRENGTH PROPERTIES							
E_0	3,842	3,874	4,022	....	3,957	....	F_0	59,540	31,110	55,360	56,570	....		
E_{90}	1,305	917	861	....	927	....	F_{90}	9,810	7,160	10,080	10,070	....		
E_{45}	1,732	2,063	1,591	....	1,607	....	F_{45}	20,020	8,920	15,100	16,060	....		

[1]Initial straight-line portion (lower slope) of load-deformation curve.

[2]Second straight-line portion (upper slope) of load-deformation curve.

Report No. 1853

Table 8.--Computed values of stress-strain ratios for tensile specimens of panel 5.

Phase of loading cycle	Stress-strain ratio value (1,000 p.s.i.)							
	Stress direction with respect to axis of reference --							
	0°	30°	45°	60°	90°	120°	135°	150°
	0° ANGLE BETWEEN STRAIN AND STRESS DIRECTIONS							
Initial	3,511	1,829	1,403	1,296	1,672	2,022	2,120	2,464
Secondary	3,342	2,717	2,147	1,643	1,315	1,996	2,833	3,568
Unloading	3,560	1,822	1,330	1,138	1,296	1,919	2,290	2,775
Reloading	3,524	1,794	1,321	1,149	1,346	1,926	2,233	2,679
	90° ANGLE BETWEEN STRAIN AND STRESS DIRECTIONS							
Initial	-15,380	-6,936	-4,633	-4,714	-15,380	-6,936	-4,633	-4,714
Secondary	159,944	9,833	7,883	10,904	159,944	9,833	7,883	10,904
Unloading	-24,914	-20,428	-9,241	-7,494	-24,914	-20,428	-9,241	-7,494
Reloading	-21,736	-14,078	-7,401	-6,467	-21,736	-14,078	-7,401	-6,467
	45° ANGLE BETWEEN STRAIN AND STRESS DIRECTIONS							
Initial	7,634	2,603	2,731	3,681	5,986	6,168	11,257	74,278
Secondary	5,708	3,339	2,396	2,036	2,861	7,245	7,673	6,439
Unloading	6,646	2,225	2,027	2,302	4,200	6,929	11,071	24,070
Reloading	6,762	2,253	2,110	2,474	4,488	6,721	11,125	29,275
	-45° ANGLE BETWEEN STRAIN AND STRESS DIRECTIONS							
Initial	11,257	54,383	7,634	3,476	2,731	5,311	5,986	5,548
Secondary	7,673	5,876	5,708	4,778	2,396	2,152	2,861	4,615
Unloading	11,071	19,807	6,646	3,216	2,027	3,050	4,200	5,396
Reloading	11,125	23,554	6,762	3,209	2,110	3,340	4,488	5,419

Table 9.--Computed values of stress-strain ratios for tensile specimens of panel 6.

Phase of loading cycle	Stress-strain ratio value (1,000 p.s.i.) — Stress direction with respect to axis of reference -- 0°	30°	45°	60°	90°	120°	135°	150°
	0° ANGLE BETWEEN STRAIN AND STRESS DIRECTIONS							
Initial	2,796	2,560	2,245	1,995	1,772	1,831	1,978	2,223
Secondary	2,524	2,571	2,491	2,046	1,311	1,478	1,917	2,440
Unloading	2,798	2,550	2,198	1,883	1,544	1,622	1,830	2,150
Reloading	2,771	2,512	2,161	1,862	1,558	1,643	1,840	2,143
	90° ANGLE BETWEEN STRAIN AND STRESS DIRECTIONS							
Initial	-8,751	-8,223	-7,759	-7,762	-8,751	-8,223	-7,759	-7,762
Secondary	-9,956	-18,587	57,608	33,764	-9,956	-18,587	57,608	33,764
Unloading	-9,840	-9,674	-10,026	-10,303	-9,840	-9,674	-10,026	-10,303
Reloading	-9,739	-9,555	-9,583	-9,690	-9,739	-9,555	-9,583	-9,690
	45° ANGLE BETWEEN STRAIN AND STRESS DIRECTIONS							
Initial	9,757	5,552	4,670	4,270	4,670	5,453	7,098	9,611
Secondary	6,026	6,378	3,956	2,628	3,956	5,815	7,703	6,566
Unloading	9,204	5,177	4,056	3,445	4,056	4,937	6,796	9,200
Reloading	9,112	5,056	4,023	3,487	4,023	4,963	6,737	9,123
	-45° ANGLE BETWEEN STRAIN AND STRESS DIRECTIONS							
Initial	7,098	11,252	9,757	7,239	4,240	4,149	4,240	4,608
Secondary	7,703	5,604	6,026	7,251	2,443	2,219	2,443	3,482
Unloading	6,796	10,463	9,204	6,961	3,337	3,219	3,337	3,856
Reloading	6,737	10,451	9,112	6,794	3,441	3,307	3,441	3,940

Table 10.--Computed strength values for tensile specimens of panel 5.

Angle of loading	Number of laminations	Warp direction[1]	Tensile strength: Loading-cycle phases -- Initial	Secondary	Unloading	Reloading
			P.s.i.	P.s.i.	P.s.i.	P.s.i.
0°	9	0°	42,927	41,388	42,122	42,213
	2	140°	6,097	2,080	5,696	5,894
	2	110°	4,053	3,857	6,152	5,668
Total			53,077	47,325	53,970	53,775
30°	9	0°	13,098	9,294	11,683	11,996
	2	140°	1,817	6,354	2,922	2,596
	2	110°	2,101	2,806	2,663	2,586
Total			17,016	18,454	17,268	17,178
45°	9	0°	9,345	8,042	9,064	9,157
	2	140°	1,466	3,131	2,259	2,036
	2	110°	1,905	1,474	2,008	2,035
Total			12,716	12,647	13,331	13,228
60°	9	0°	7,899	8,637	8,379	8,302
	2	140°	1,424	1,374	1,984	1,853
	2	110°	2,010	1,100	1,820	1,900
Total			11,333	11,111	12,183	12,055
90°	9	0°	8,162	19,351	10,470	9,860
	2	140°	2,227	842	2,120	2,188
	2	110°	3,731	1,132	2,461	2,699
Total			14,120	21,325	15,051	14,747
120°	9	0°	12,057	13,679	14,419	13,860
	2	140°	4,708	1,212	3,528	3,829
	2	110°	5,195	3,202	5,195	5,210
Total			21,960	18,093	23,142	22,899
135°	9	0°	15,065	11,901	15,138	15,167
	2	140°	4,931	2,366	5,056	5,126
	2	110°	4,365	8,155	4,596	4,524
Total			24,361	22,422	24,790	24,817
150°	9	0°	18,986	14,025	17,583	17,886
	2	140°	5,496	12,090	6,793	6,486
	2	110°	4,348	3,428	4,120	4,167
Total			28,830	29,543	28,496	28,539

[1]Panel 5 consisted of 13 laminations of 143-114 fabric with the warp direction of 9 laminations making an angle of 0° with the axis of reference, 2 an angle of 140°, and 2 an angle of 110°.

Table 11. Computed strength values for tensile specimens of panel 6.

Angle of loading	Number of laminations	Warp direction[1]	Tensile strength — Loading-cycle phases -- Initial	Secondary	Unloading	Reloading
			P.s.i.	P.s.i.	P.s.i.	P.s.i.
0°	4	10°	14,871	8,901	13,571	13,930
	3	0°	9,869	11,086	10,454	10,425
	5	140°	16,598	14,769	16,675	16,491
Total			41,338	34,756	40,700	40,846
30°	4	10°	12,167	4,908	9,746	10,249
	3	0°	8,497	9,492	8,514	8,355
	5	140°	14,979	17,964	16,056	15,923
Total			35,643	32,364	34,316	34,527
45°	4	10°	8,784	3,417	7,290	7,630
	3	0°	7,278	9,366	7,274	7,119
	5	140°	13,088	20,661	14,226	14,067
Total			29,150	33,444	28,790	28,816
60°	4	10°	6,260	3,231	6,308	6,365
	3	0°	6,632	8,467	6,590	6,510
	5	140°	12,060	14,335	12,282	12,222
Total			24,952	26,033	25,180	25,097
90°	4	10°	4,287	2,939	5,872	5,490
	3	0°	5,804	5,671	5,635	5,709
	5	140°	11,344	8,392	9,989	10,100
Total			21,435	17,002	21,496	21,299
120°	4	10°	4,634	4,800	6,006	5,729
	3	0°	6,209	5,720	5,744	5,822
	5	140°	10,782	9,300	10,168	10,211
Total			21,625	19,820	21,918	21,762
135°	4	10°	5,782	3,475	6,239	6,273
	3	0°	6,573	6,820	6,188	6,198
	5	140°	10,763	12,784	11,135	11,031
Total			23,118	23,079	23,562	23,502
150°	4	10°	8,003	3,352	7,016	7,360
	3	0°	7,446	9,134	7,251	7,195
	5	140°	11,638	18,435	12,670	12,419
Total			27,087	30,921	26,937	26,974

[1]Panel 6 was of 12 laminations consisting of 4, 3, and 5 laminations of 143-114, 162-114, and 187-114 fabrics respectively, with the warp direction of each fabric parallel and oriented with respect to an axis of reference as follows: 4 laminations of 143-114 at 10°, 3 laminations of 162-114 at 0°, and 5 laminations of 181-114 at 140°.

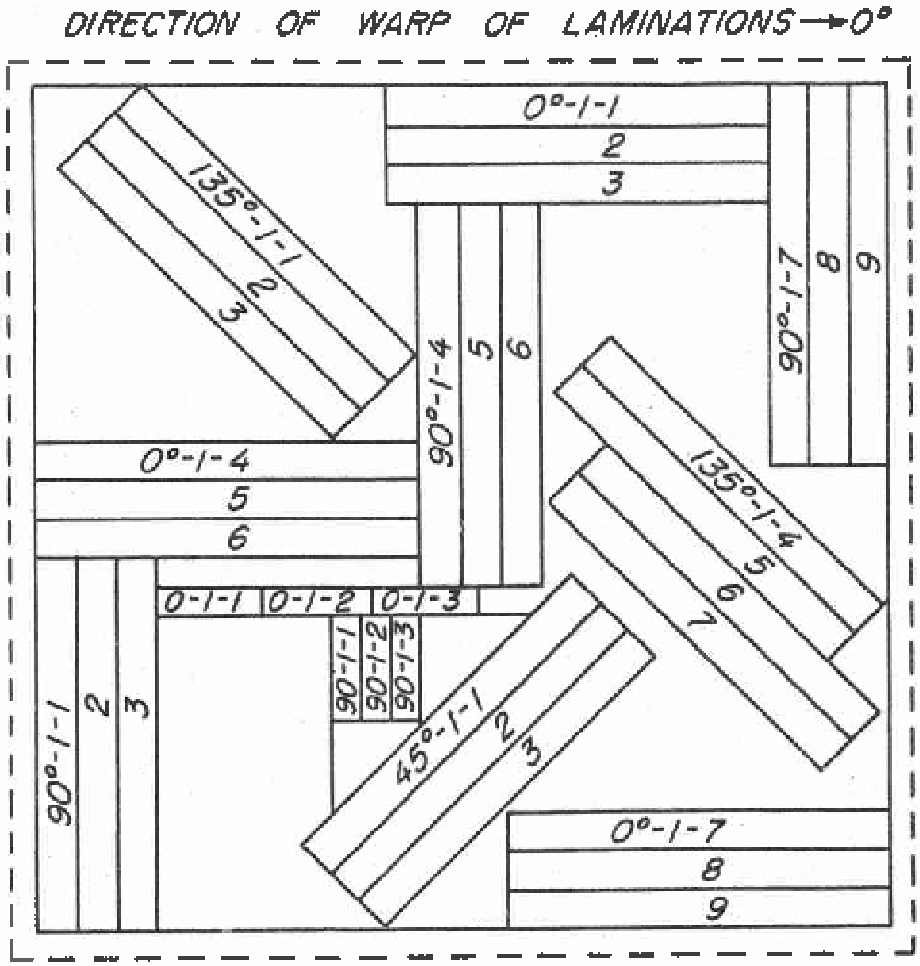

Figure 1. --Plan for cutting tension and compression specimens from 1/8- by 36- by 36-inch glass-fabric laminated panels 1, 2, and 3. Panel 1 consisted of 12 plies of fabric 143-114, panel 2 of 12 plies of fabric 181-114, and panel 3 of 8 plies of fabric 162-114, all parallel laminated.

M 106 898

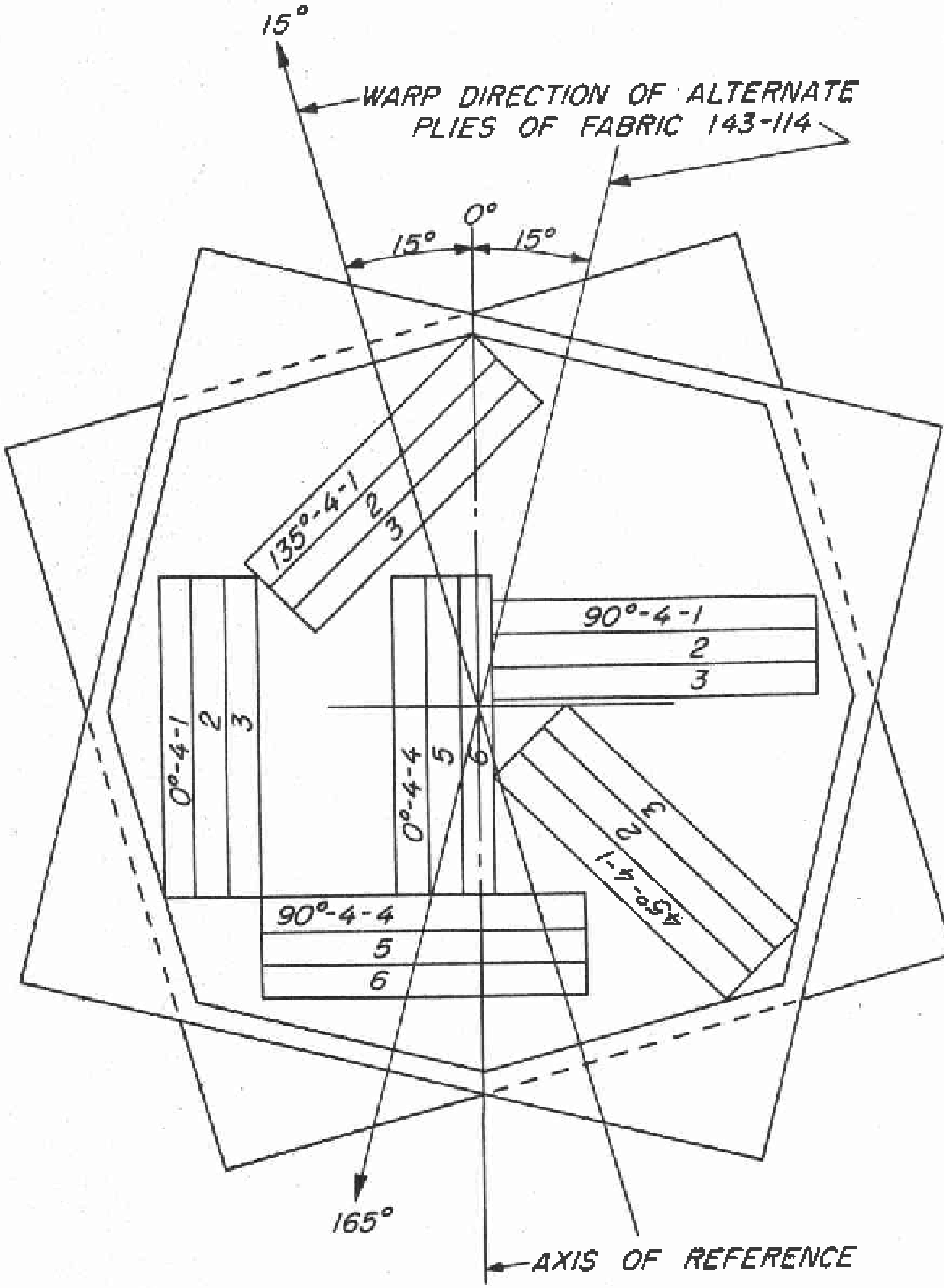

Figure 2. --Cutting diagram for tensile specimens from 1/8- by 36- by 36-inch glass-fabric laminated panel 4.

M 106 899

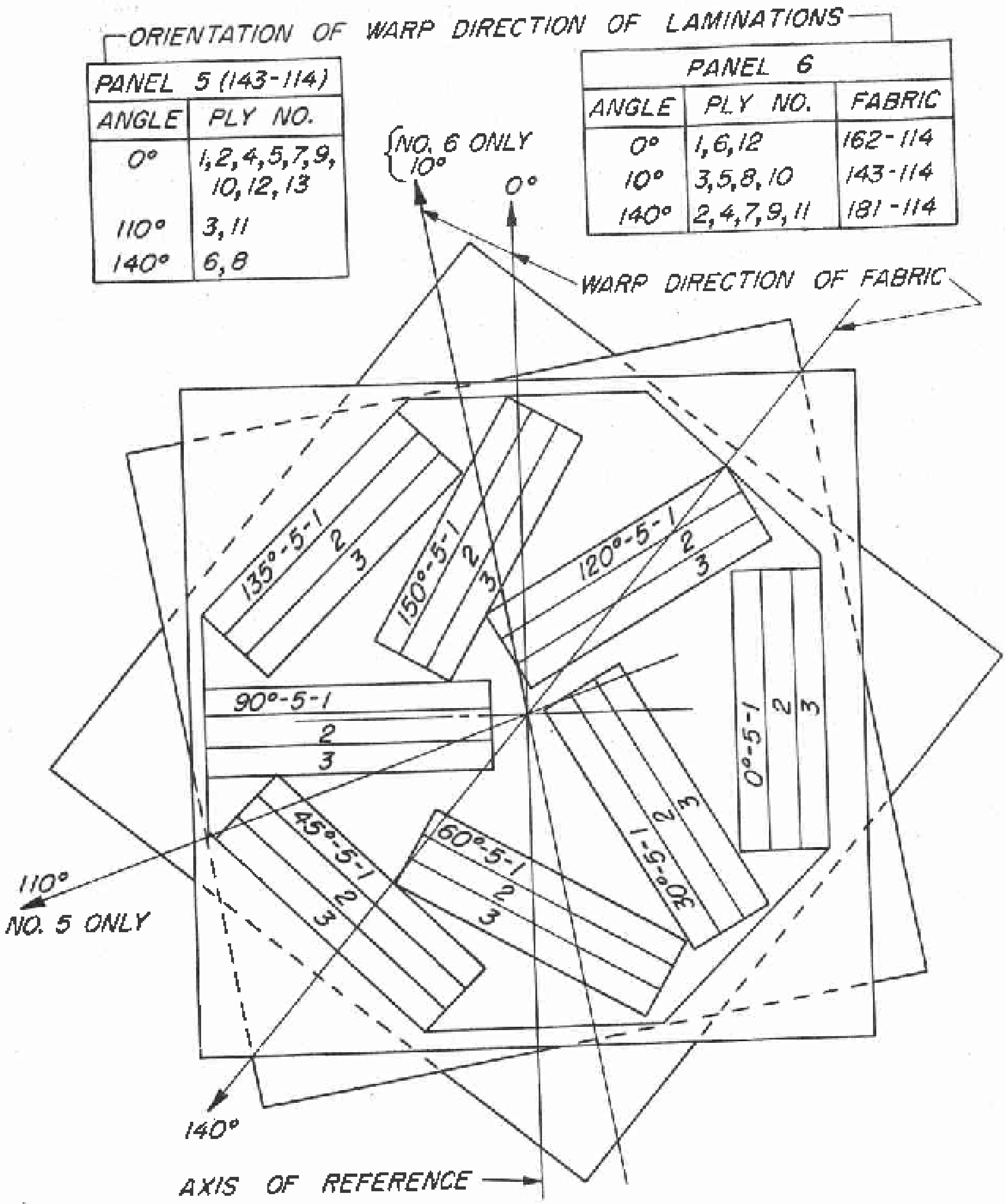

Figure 3.--Cutting diagram for glass-fabric tensile specimens from 1/8- by 36- by 36-inch panels 5 and 6.

M 106 860

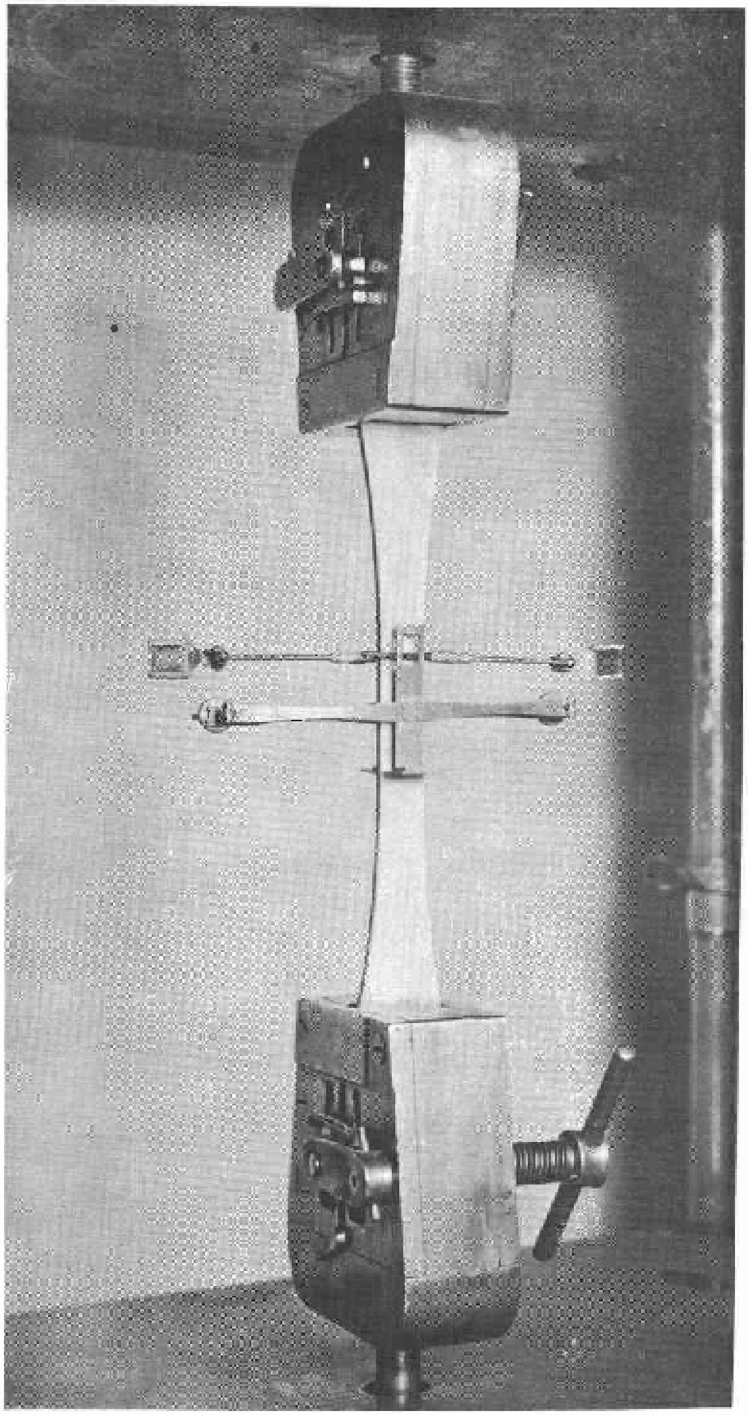

Figure 4. --Tensile test used in testing glass-fabric-laminate specimens.

Z M 80078 F

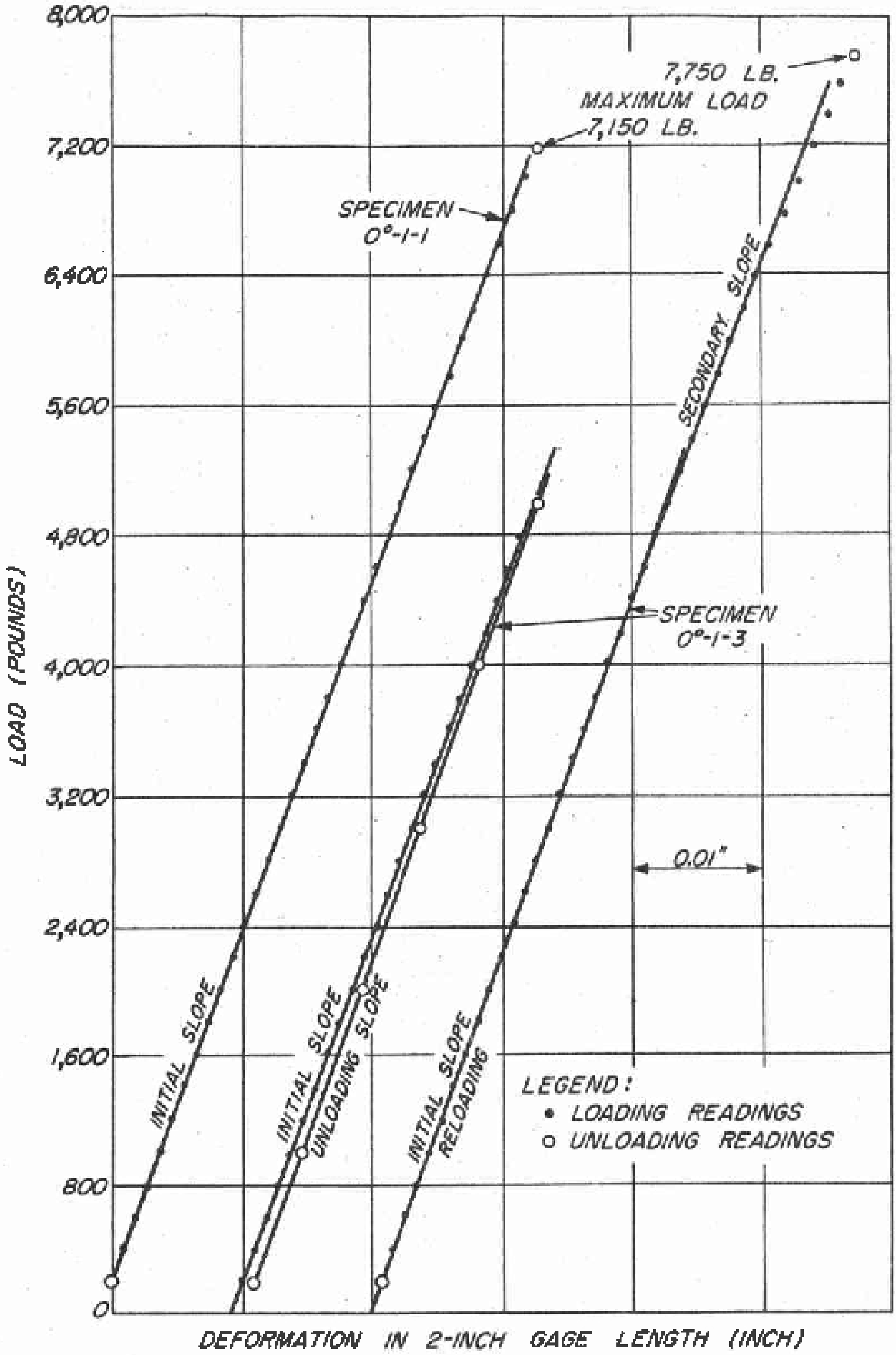

Figure 5. --Representative load-deformation curves for tension specimens of parallel-laminated panel 1, tested at 0° to the warp of the 143-114 fabric.

M 106 861

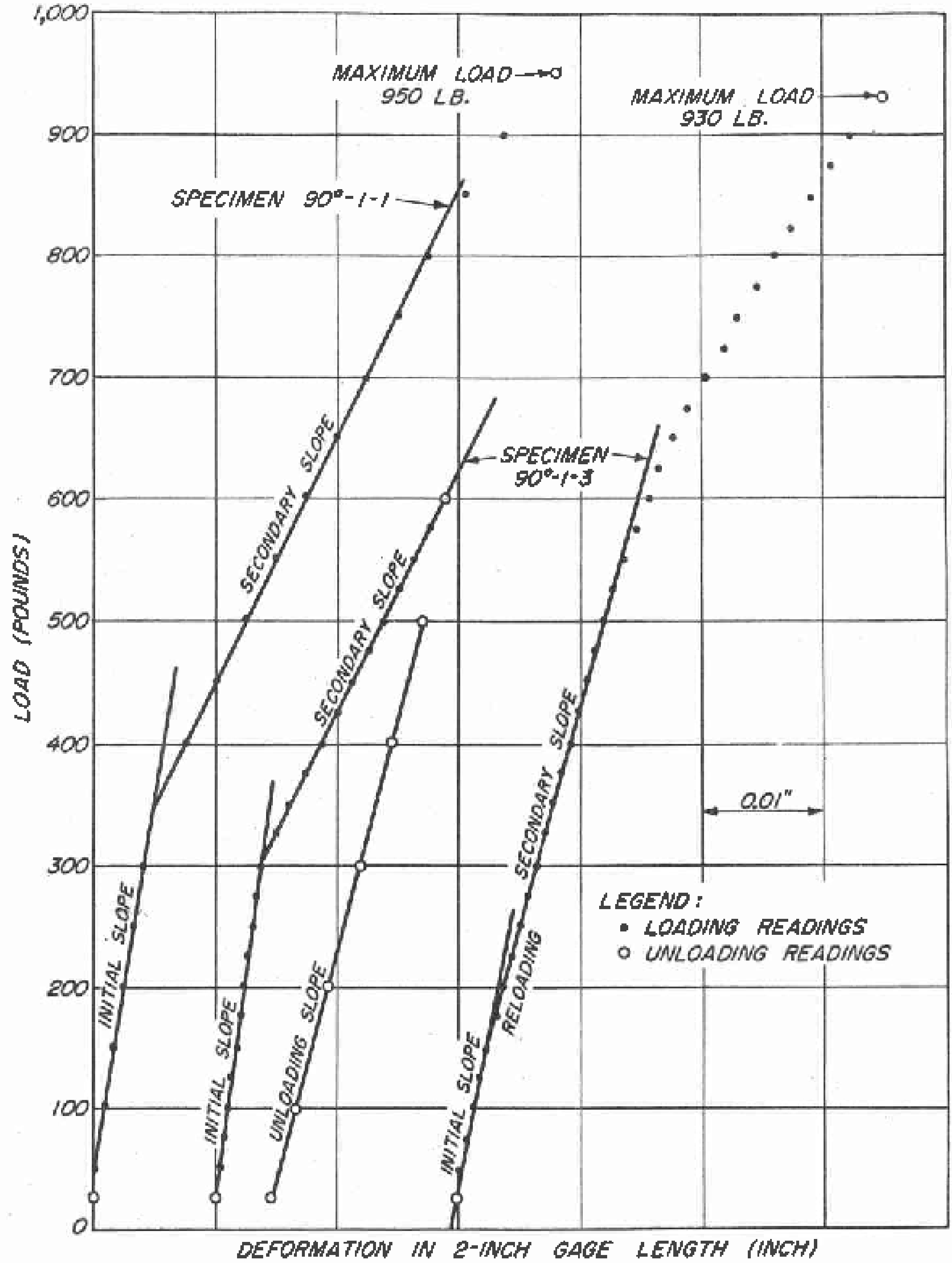

Figure 6. --Representative load-deformation curves for tension specimens of parallel-laminated panel 1, tested at 90° to the warp of the 143-114 fabric.

M 106 862

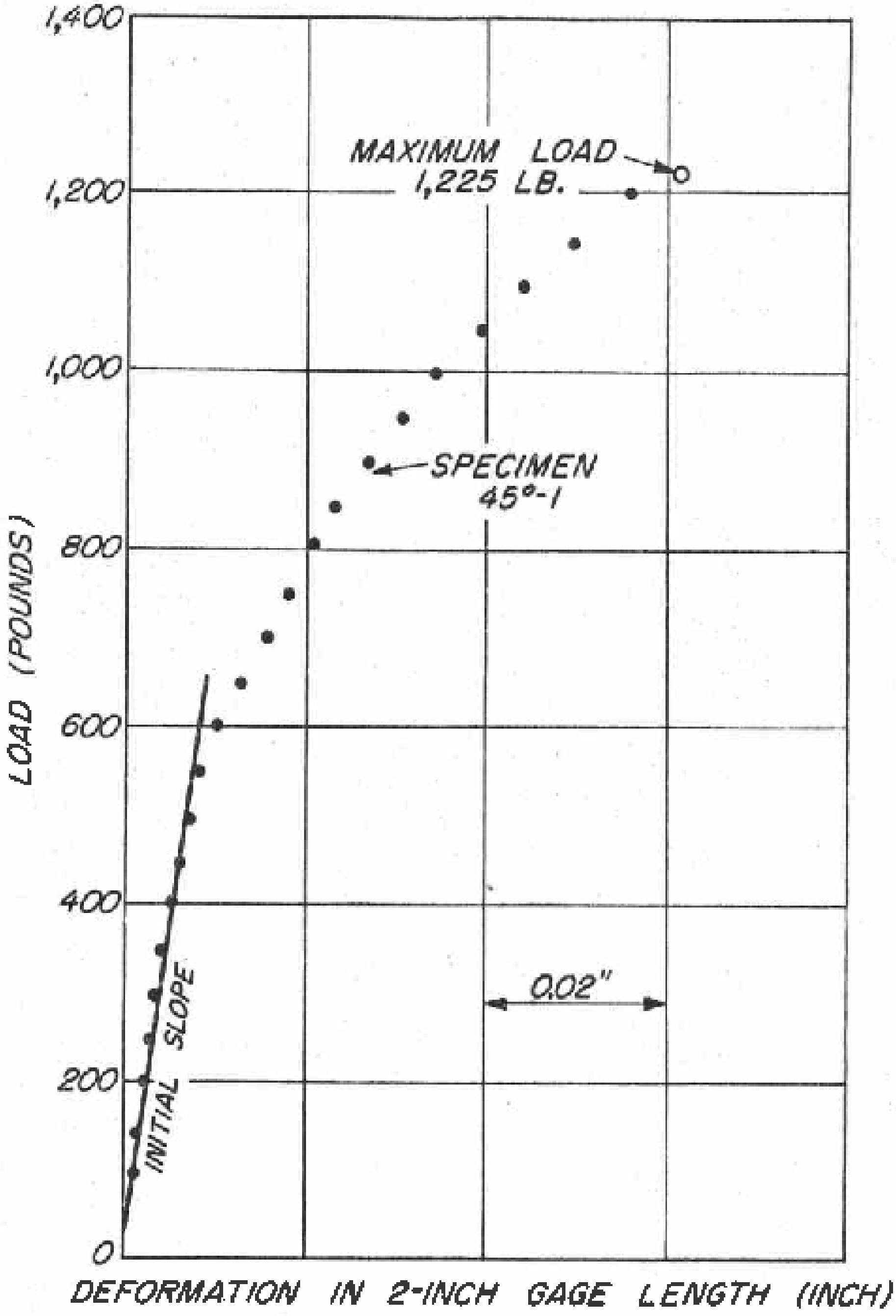

Figure 7. --Representative load-deformation curve for tension specimens of parallel-laminated panel 1, tested at 45° to the warp of the 143-114 fabric.

M 106 863

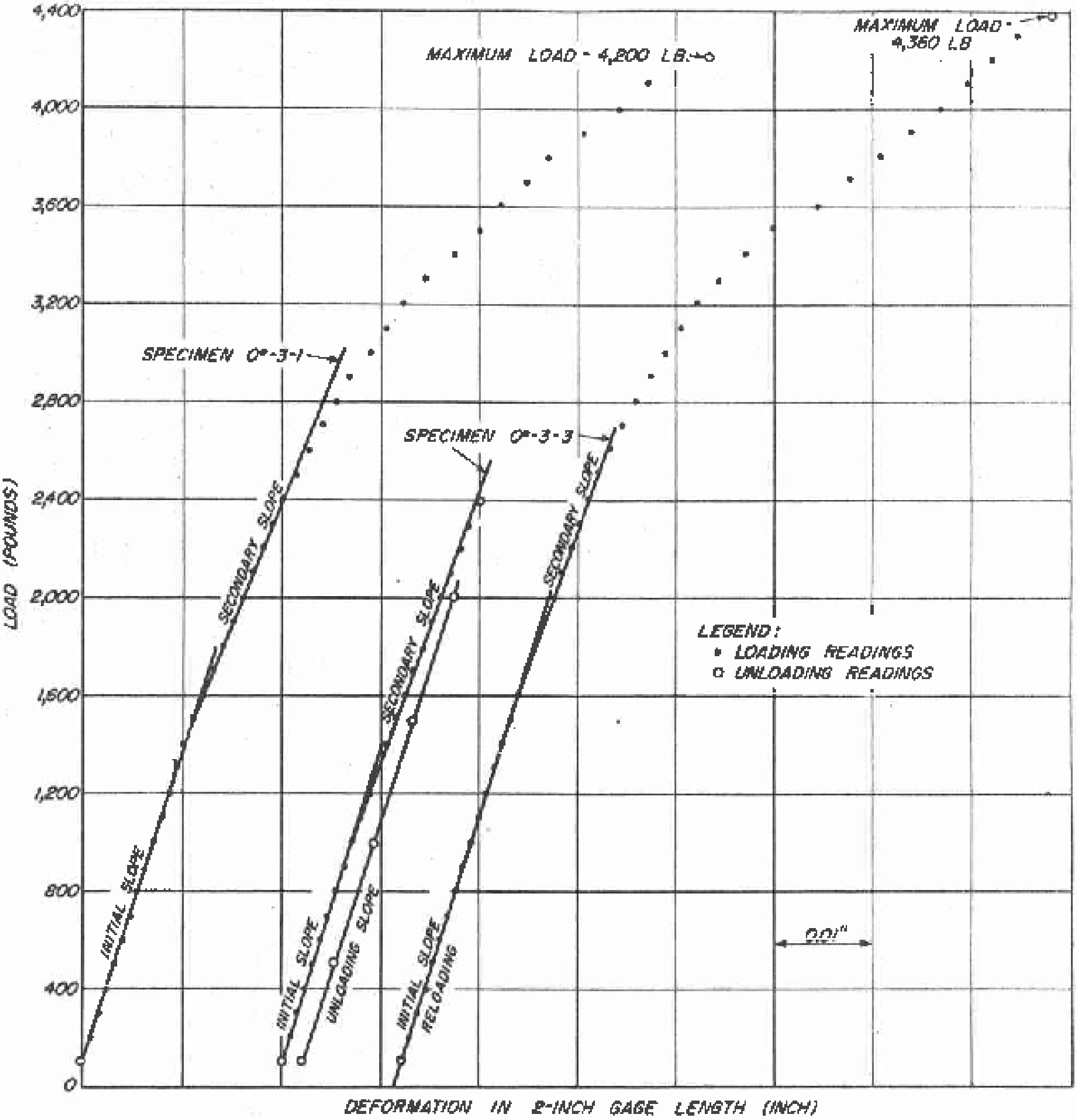

Figure 8. --Representative load-deformation curves for tension specimens of parallel-laminated panel 3, tested at 0° to the warp of the 162-114 fabric.

M 106 864

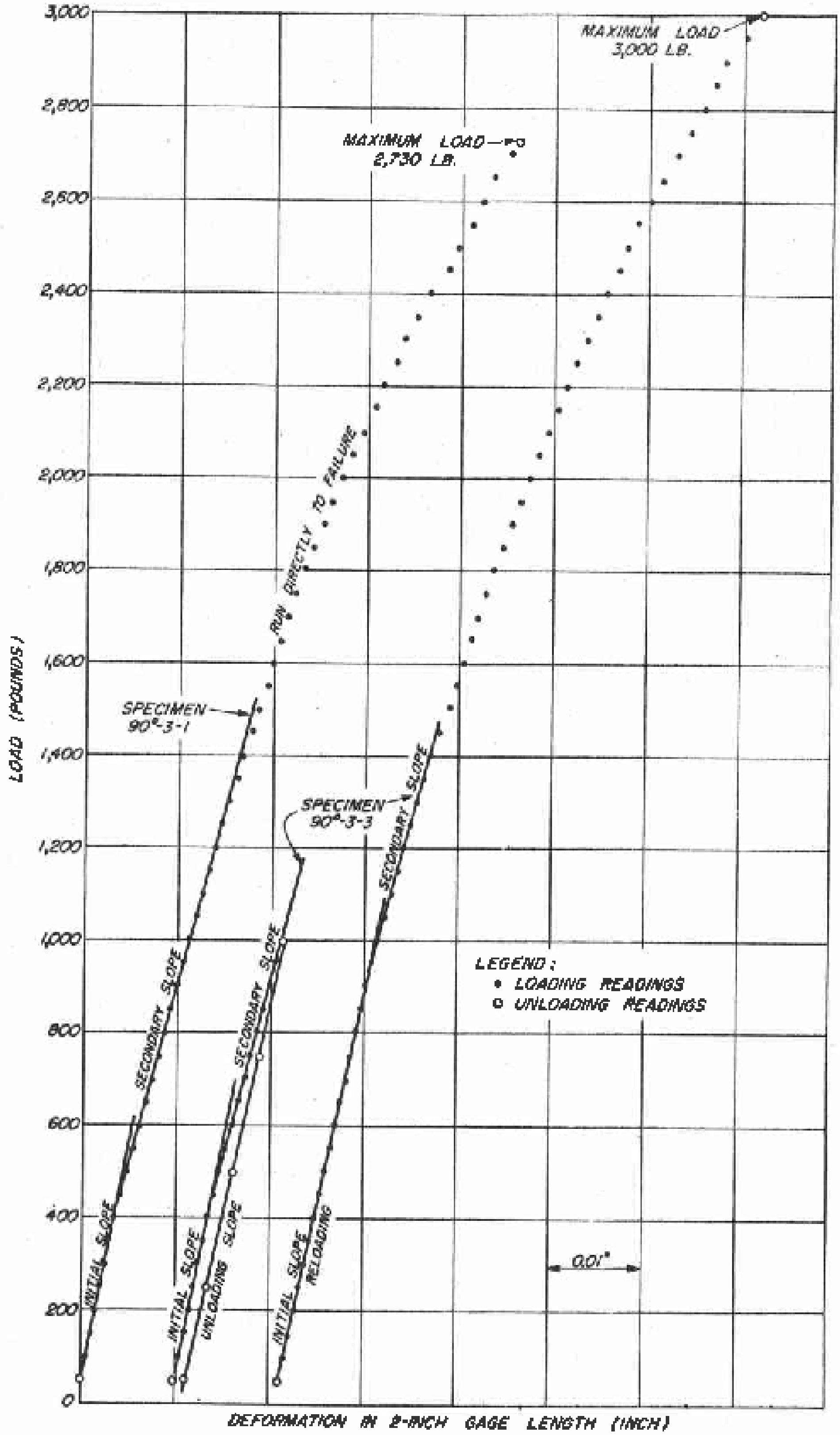

Figure 9. --Representative load-deformation curves for tension specimens of parallel-laminated panel 3, tested at 90° to the warp of the 162-114 fabric.

M 106 865

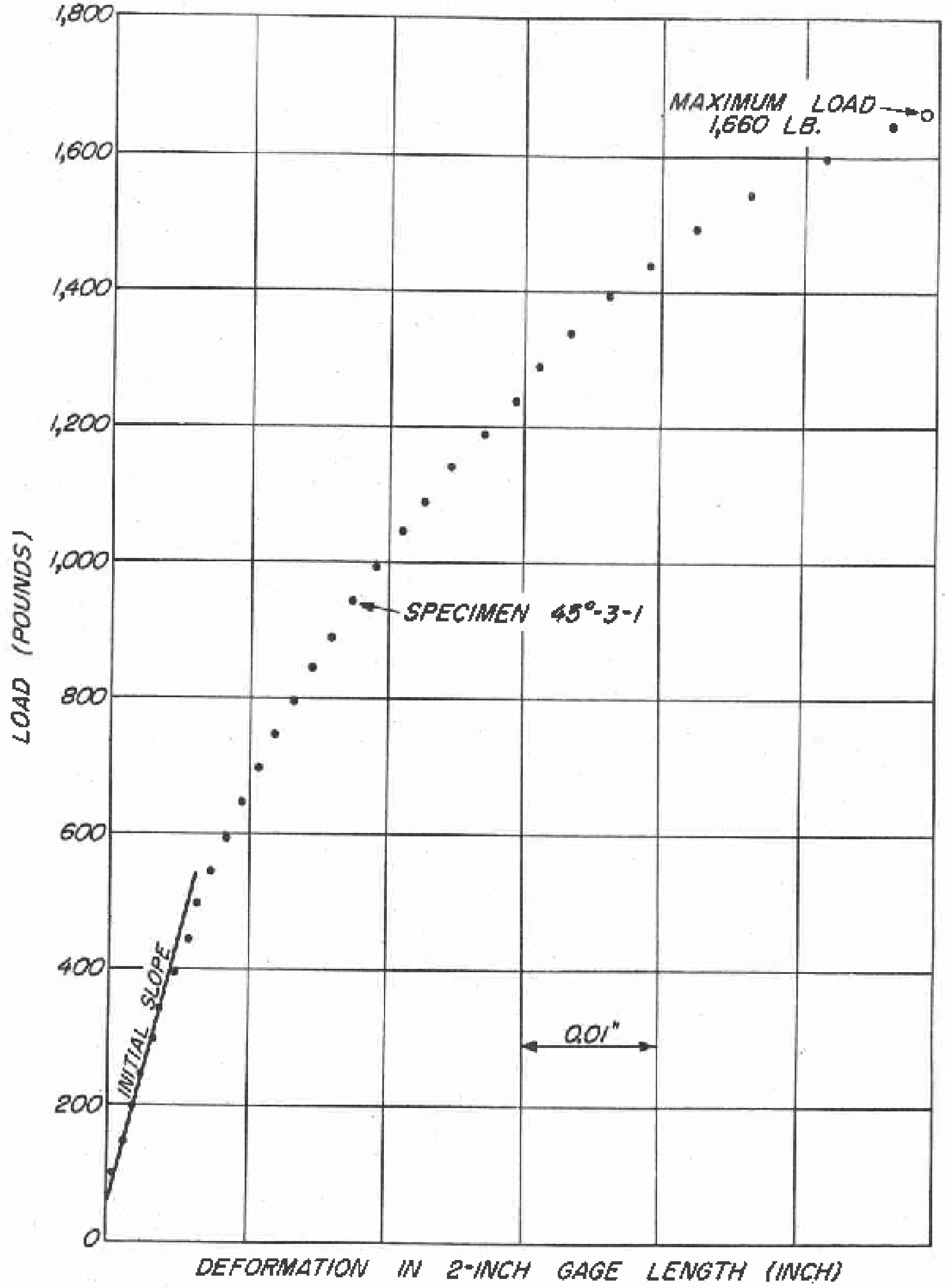

Figure 10. --Representative load-deformation curve for tension specimens of parallel-laminated panel 3, tested at 45° to the warp of the 162-114 fabric.

M 106 866

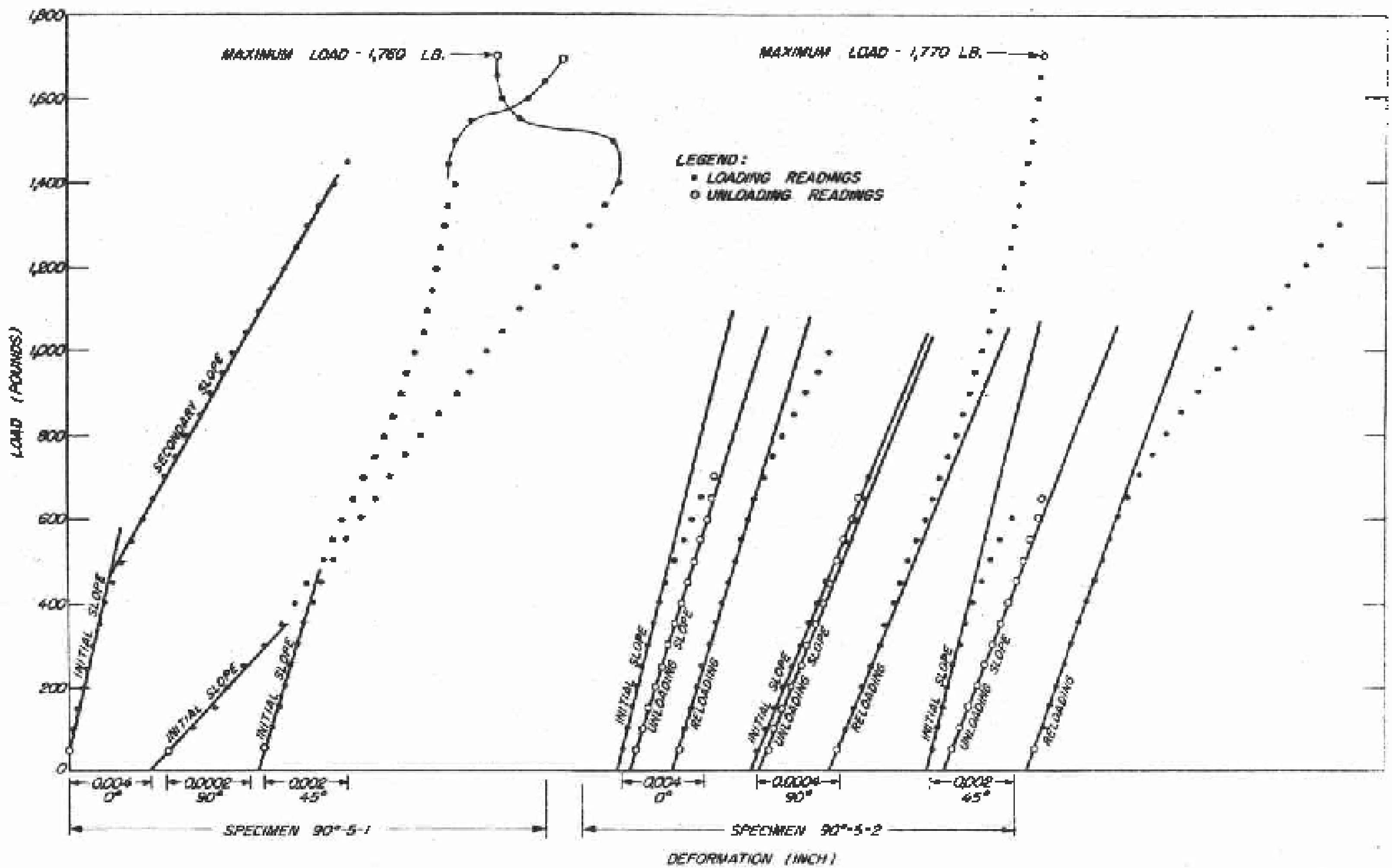

Figure 11. --Representative load-deformation curves for tension specimens of 143-114 fabric tested at 90° to the axis of reference for panel 5. Load-deformation data from the 0°, 90°, and 45° elements of Rosette-type strain gages are shown. Specimen 90°-5-1 tested directly to failure; specimen 90°-5-2 preloaded, then reloaded to failure.

M 106 867

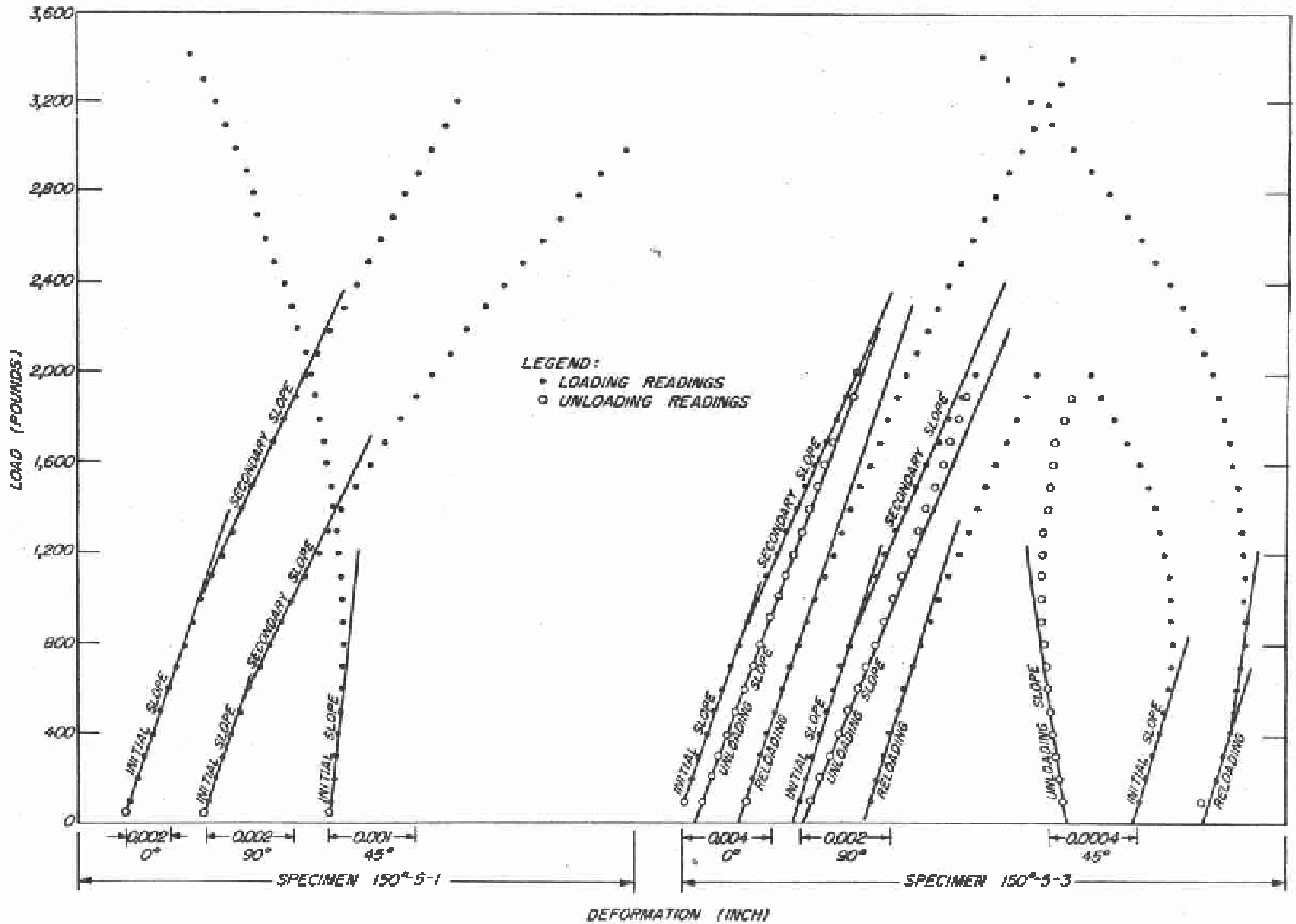

Figure 12. --Representative load-deformation curves for tension specimens of 143-114 fabric tested at 150° to the axis of reference for panel 5. Load-deformation data from the 0°, 90°, and 45° elements of Rosette-type strain gages are shown. Specimen 150°-5-1 tested directly to failure; specimen 150°-5-3 preloaded, then reloaded to failure.

M 106 868

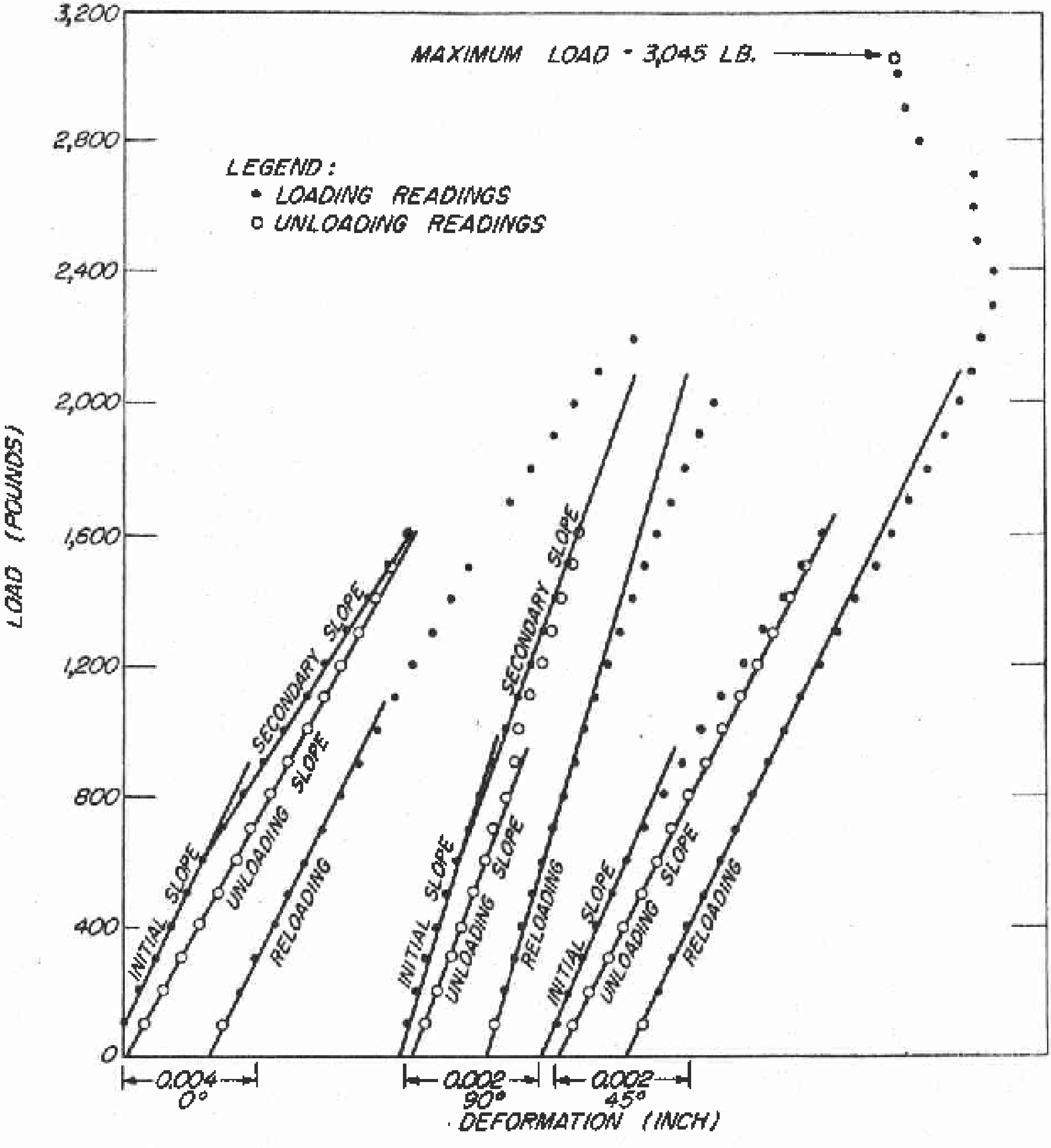

Figure 13. --Representative load-deformation curves for tension specimen (specimen 6-3) tested at 60° to the axis of reference for panel 6. Load-deformation data for the 0°, 90°, and 45° elements of Rosette-type strain gages are shown.

M 106 869

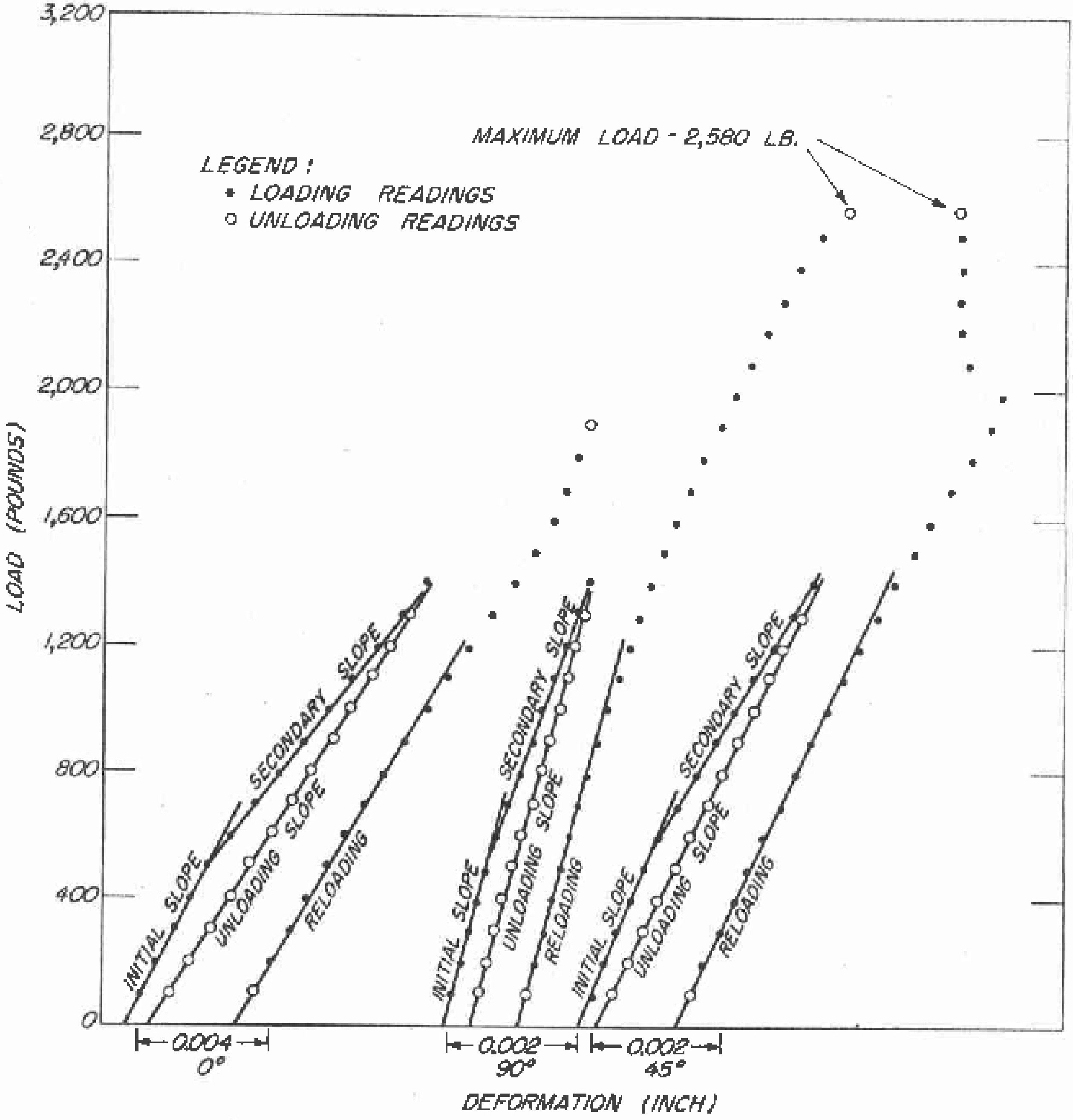

Figure 14. --Representative load-deformation curves for tension specimen (specimen 6-2) tested at 90° to axis of reference for panel 6. Load-deformation data for the 0°, 90°, and 45° elements of Rosette-type strain gages are shown.

M 106 870

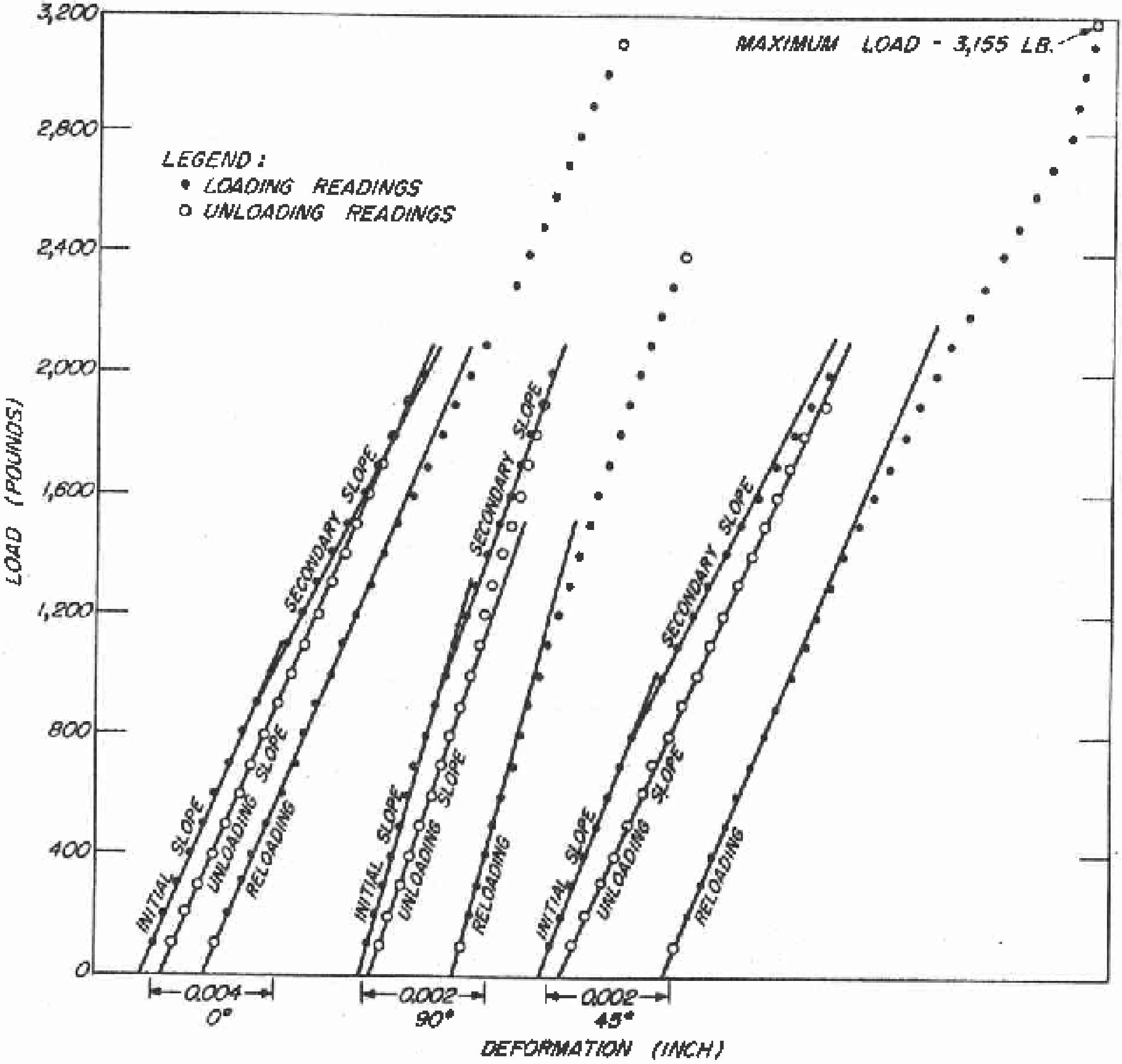

Figure 15. --Representative load-deformation curves for tension specimen (specimen 6-2) tested at 150° to axis of reference for panel 6. Load-deformation data for the 0°, 90°, and 45° elements of Rosette-type strain gages are shown.

M 106 871

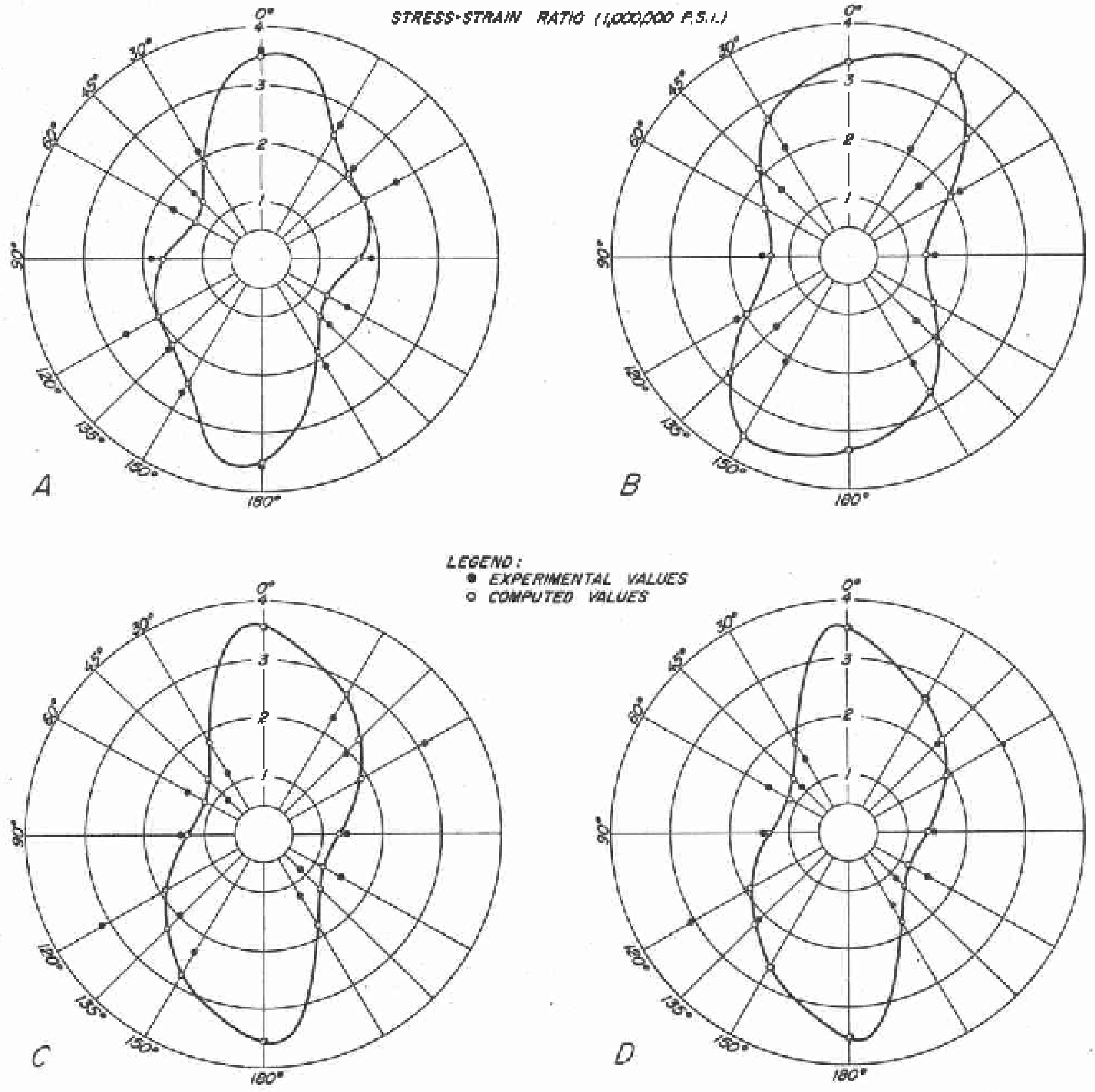

Figure 16. --Computed and experimental values of stress-strain ratios for panel 5 in the stress direction (E_0), based on elastic properties. A, initial phase of loading cycle; B, secondary phase; C, unloading phase; D, reloading phase.

M 106 872

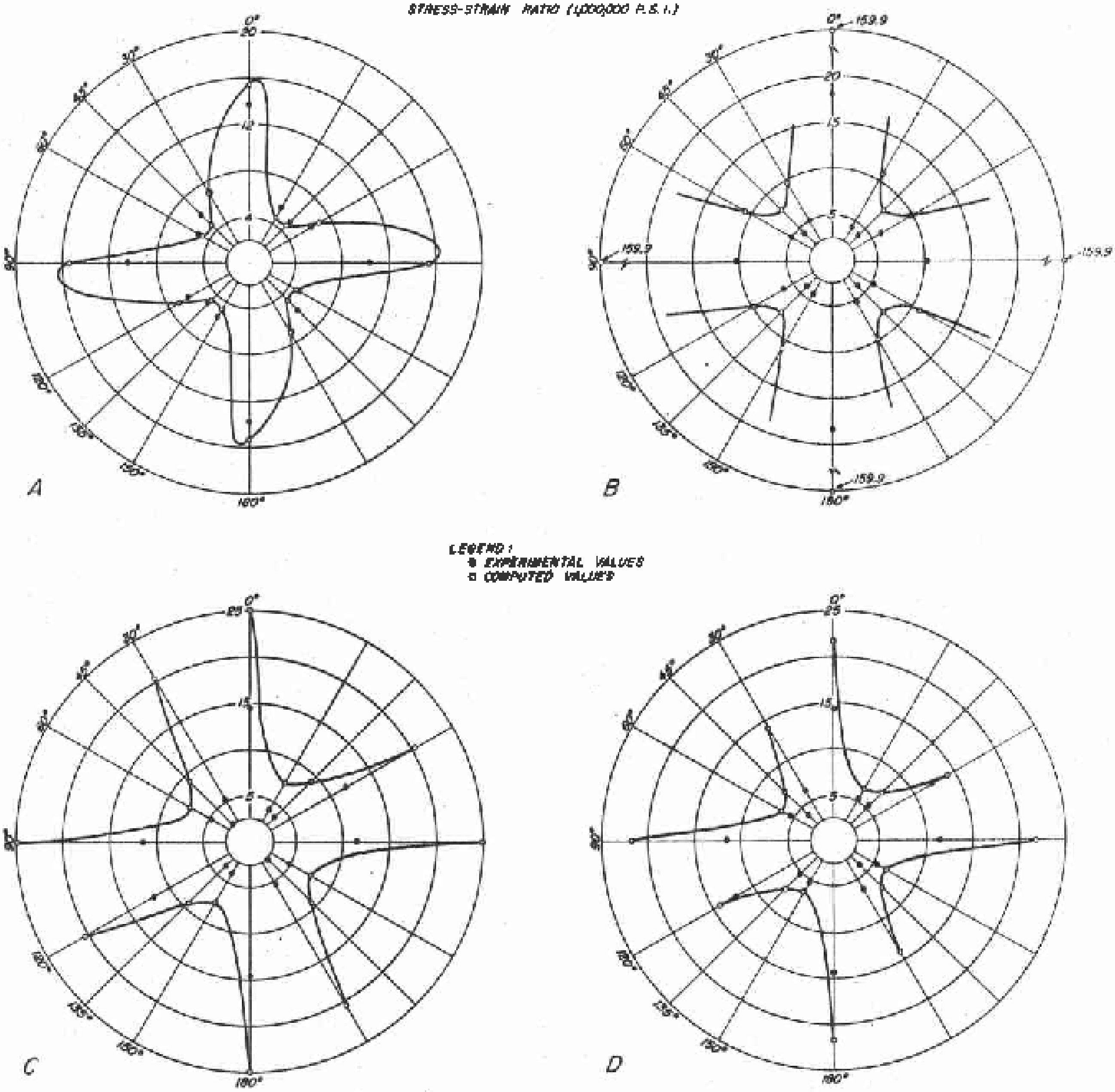

Figure 17. --Computed and experimental values of stress-strain ratios for panel 5 at 90° to the stress direction ($\underline{E_{90}}$), based on elastic properties. A, initial phase of loading cycle; B, secondary phase; C, unloading phase; D, reloading phase.

M 106 873

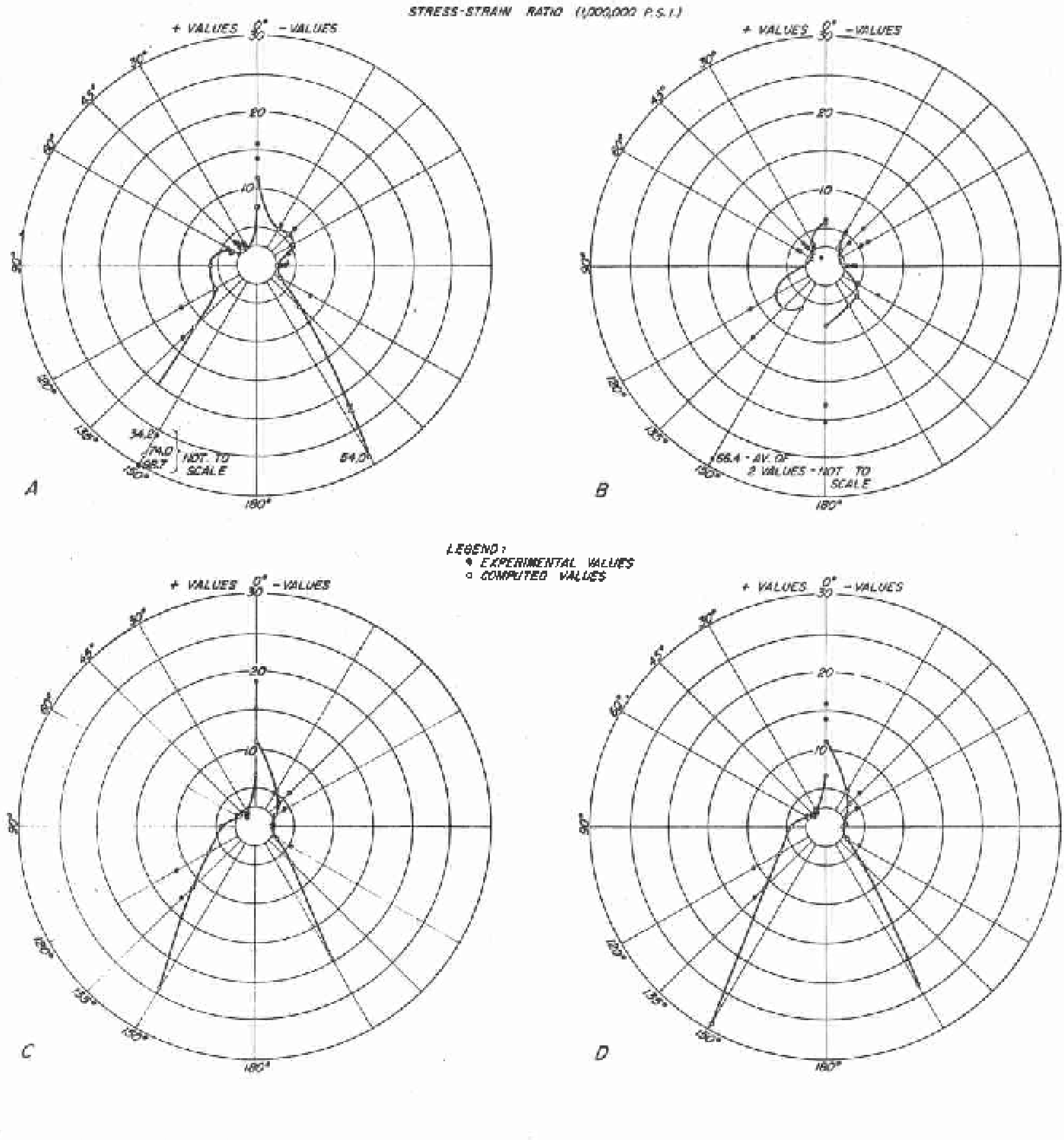

Figure 18.--Computed and experimental values of stress-strain ratios for panel 5 at plus and minus 45° to the stress direction (E_{45}), based on elastic properties. A, initial phase of loading cycle; B, secondary phase; C, unloading phase; D, reloading phase.

M 106 874

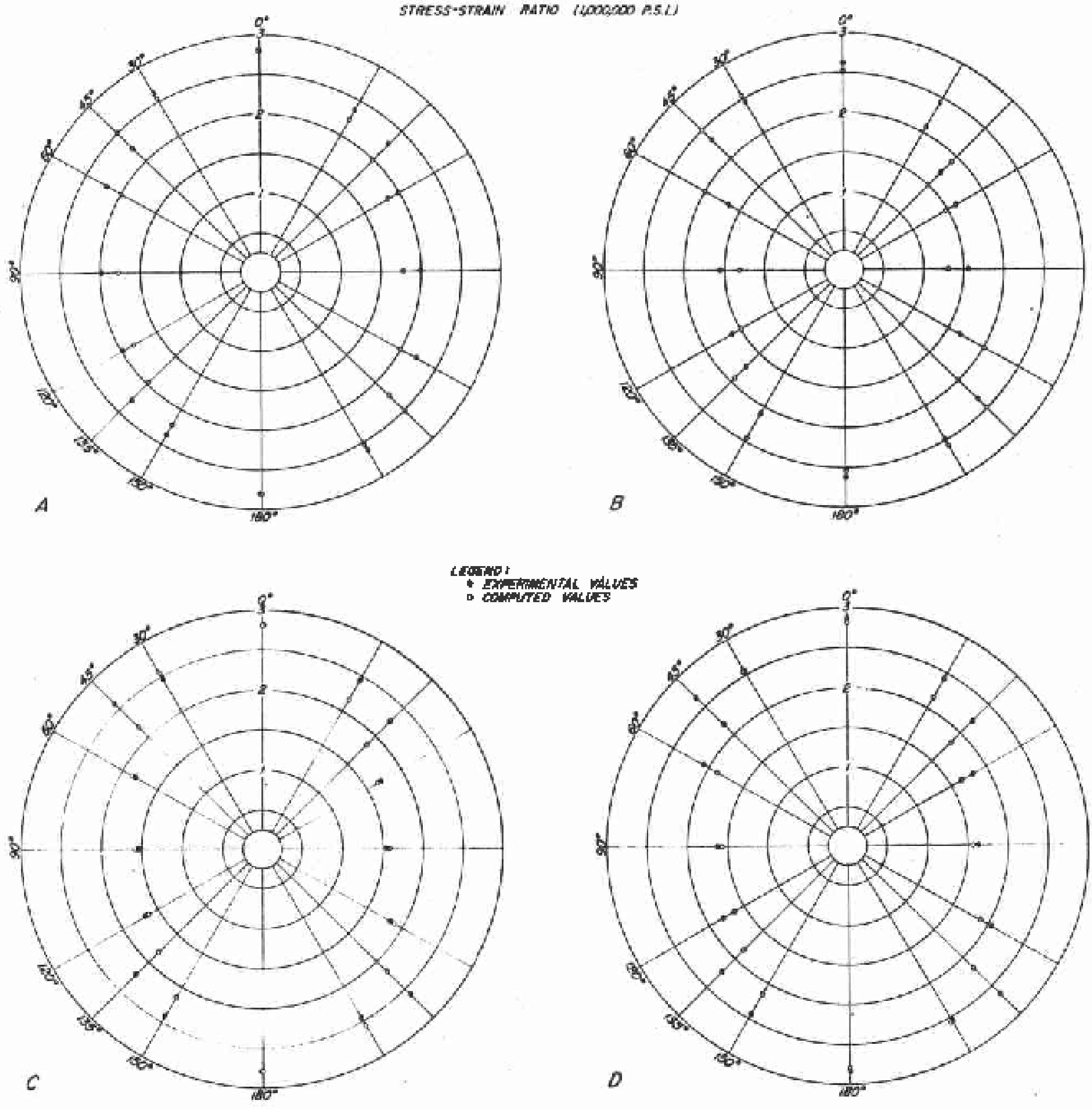

Figure 19.--Computed and experimental values of stress-strain ratios for panel 6 in the stress direction (E_0), based on elastic properties. A, initial phase of loading cycle; B, secondary phase; C, unloading phase; D, reloading phase.

M 106 875

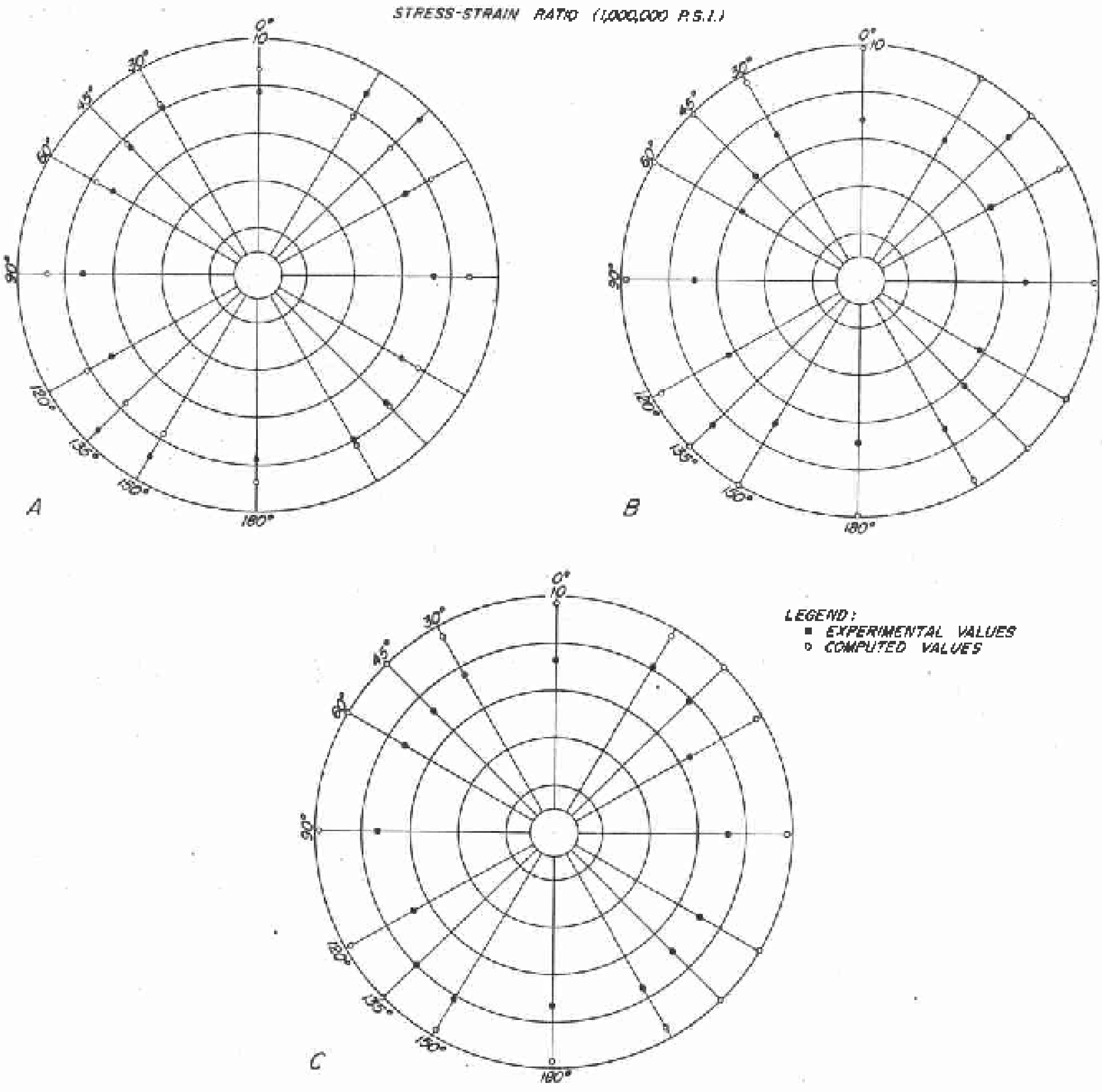

Figure 20. --Computed and experimental values of stress-strain ratios for panel 6 at 90° to the stress direction (E_{90}), based on elastic properties. A, initial phase of loading cycle; B, unloading phase; C, reloading phase.

M 106 876

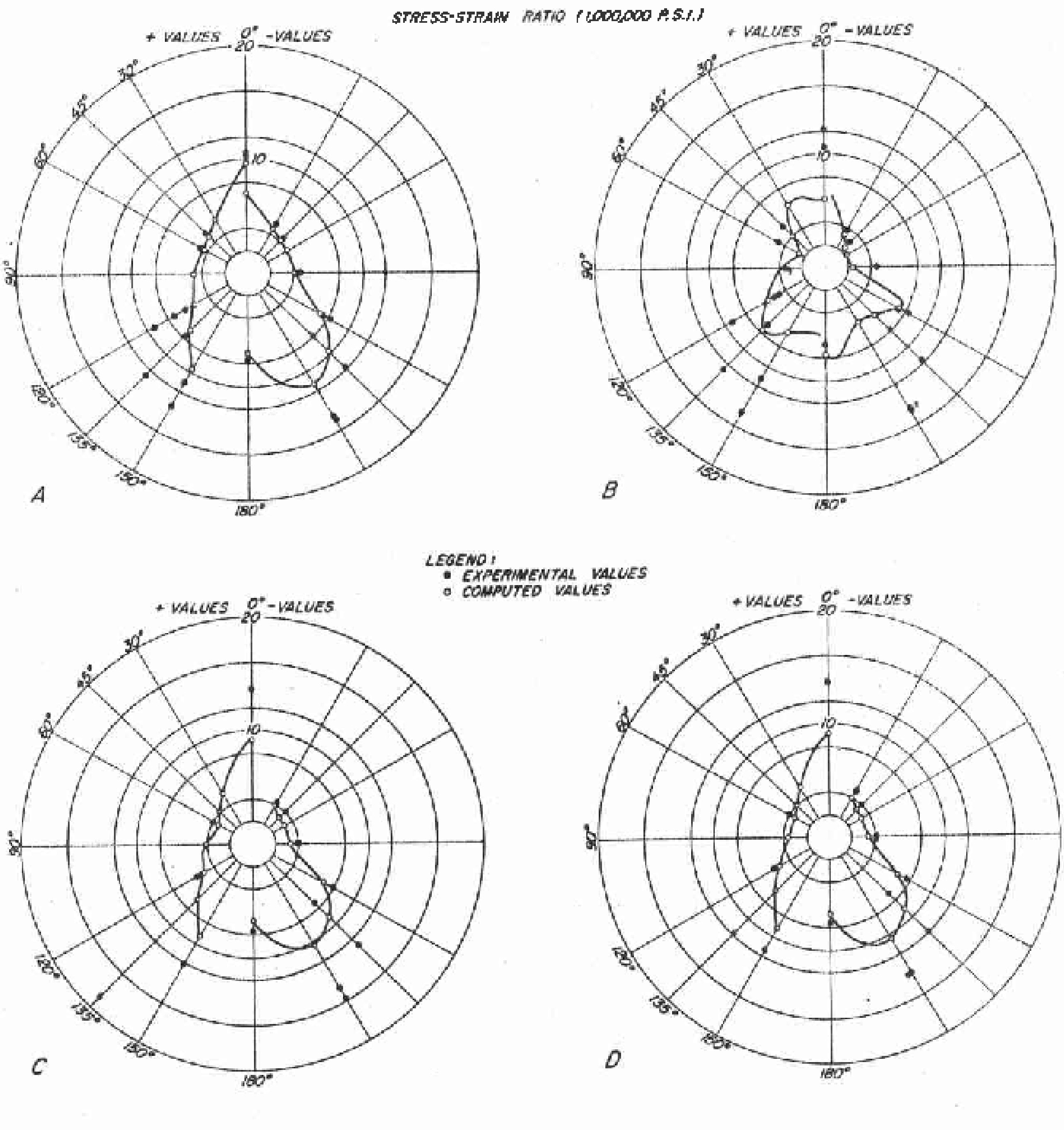

Figure 21. --Computed and experimental values of stress-strain ratios for panel 6 at plus and minus 45° to the stress direction (E_{45}), based on elastic properties. A, initial phase of loading cycle; B, secondary phase; C, unloading phase; D, reloading phase.

M 106 877

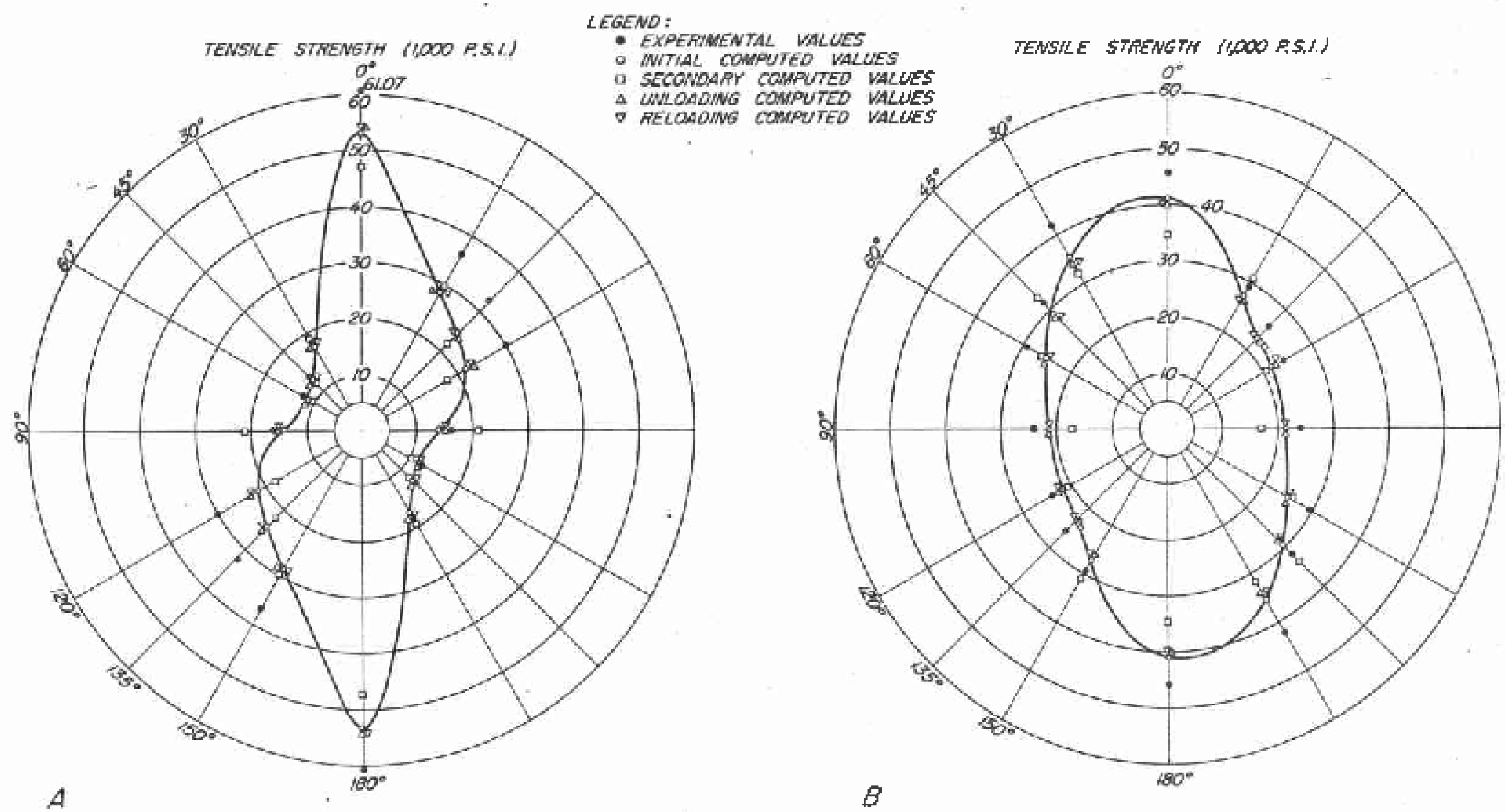

Figure 22. --Computed and experimental values of tensile strength at various angles of applied stress. A, panel 5, and B, panel 6.

M 106 878

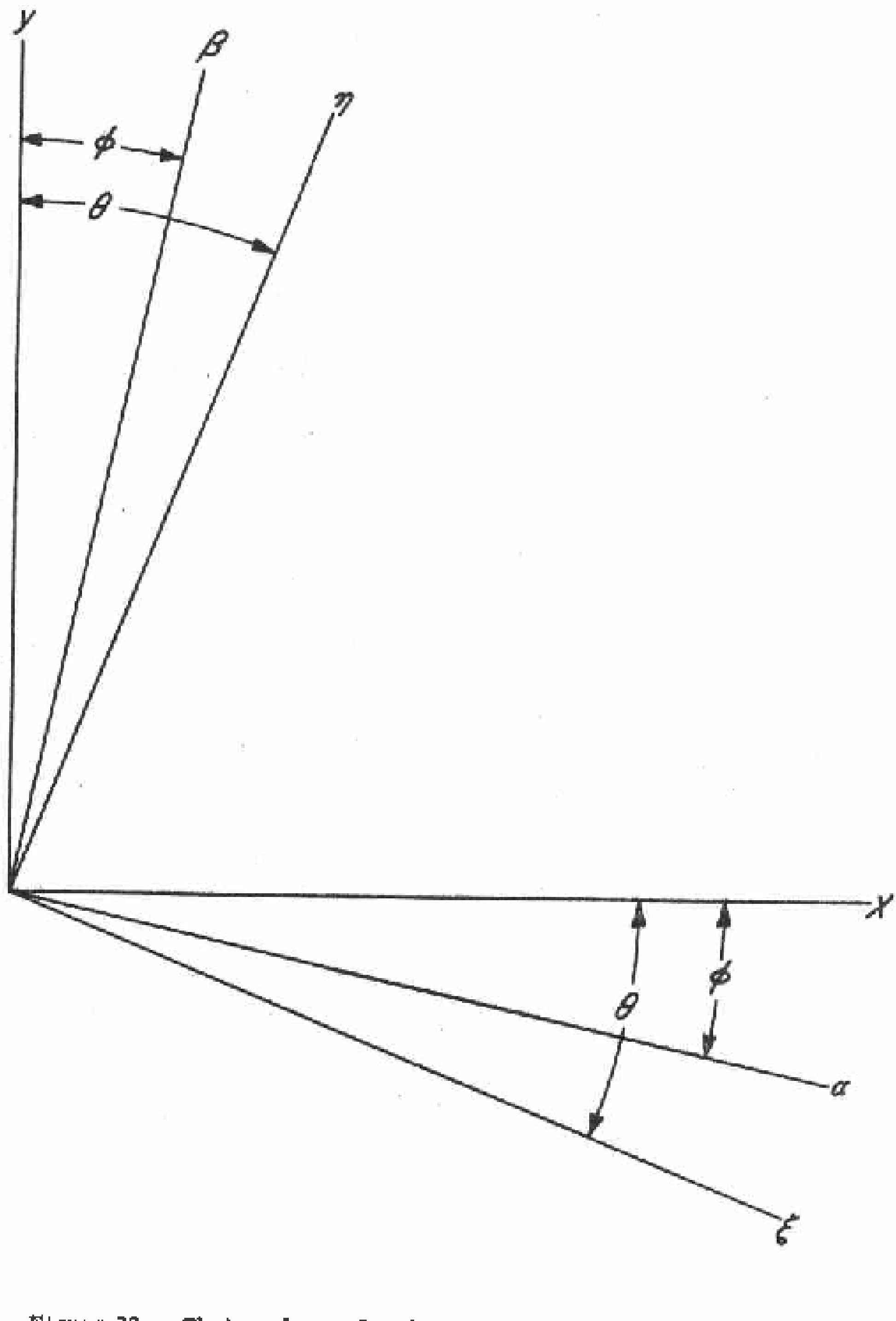

Figure 23. --Choice of axes for the mathematical analysis of the elastic properties of a laminate.

M 106 879

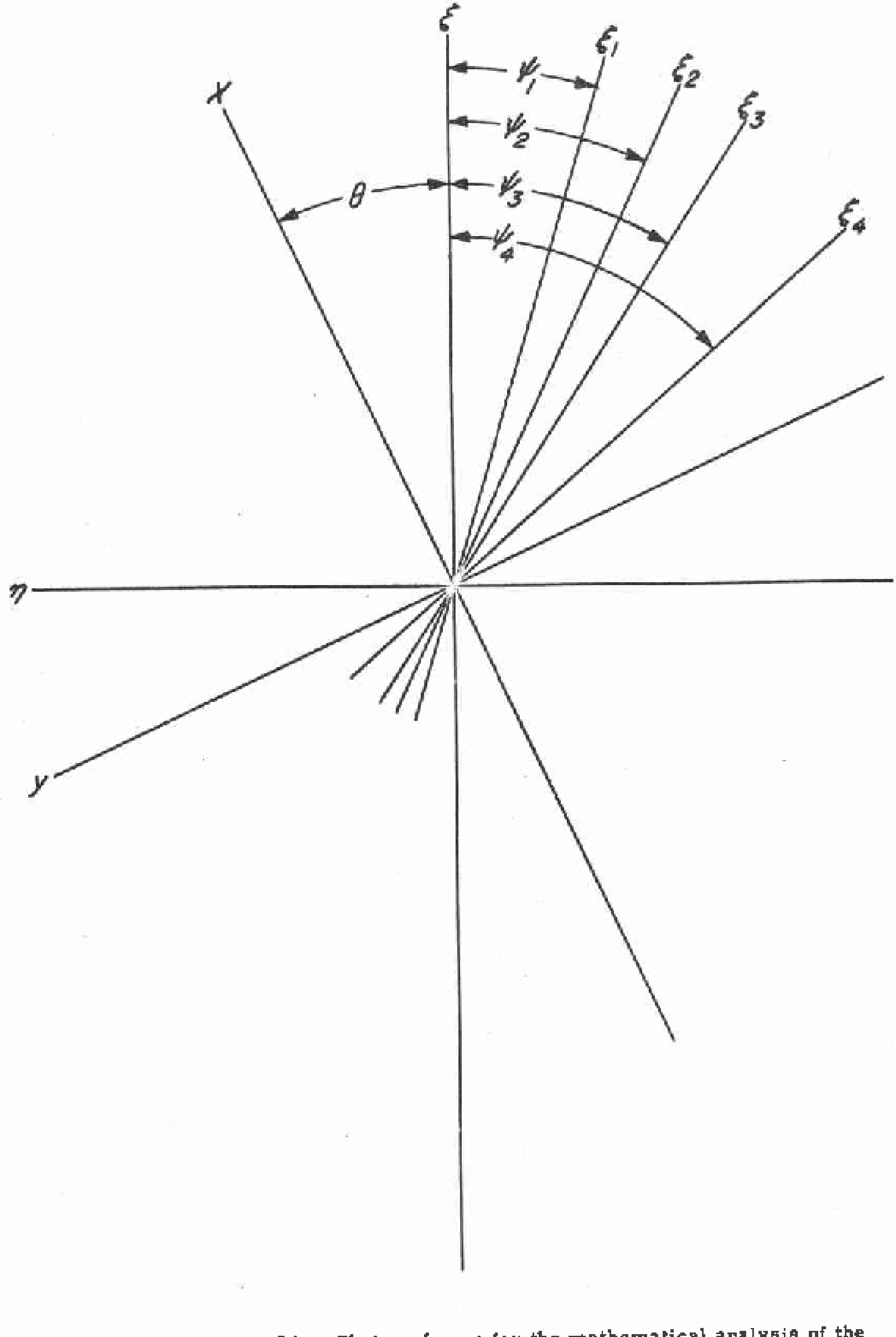

Figure 24. --Choice of axes for the mathematical analysis of the strength of a laminate.

Z M 106 880

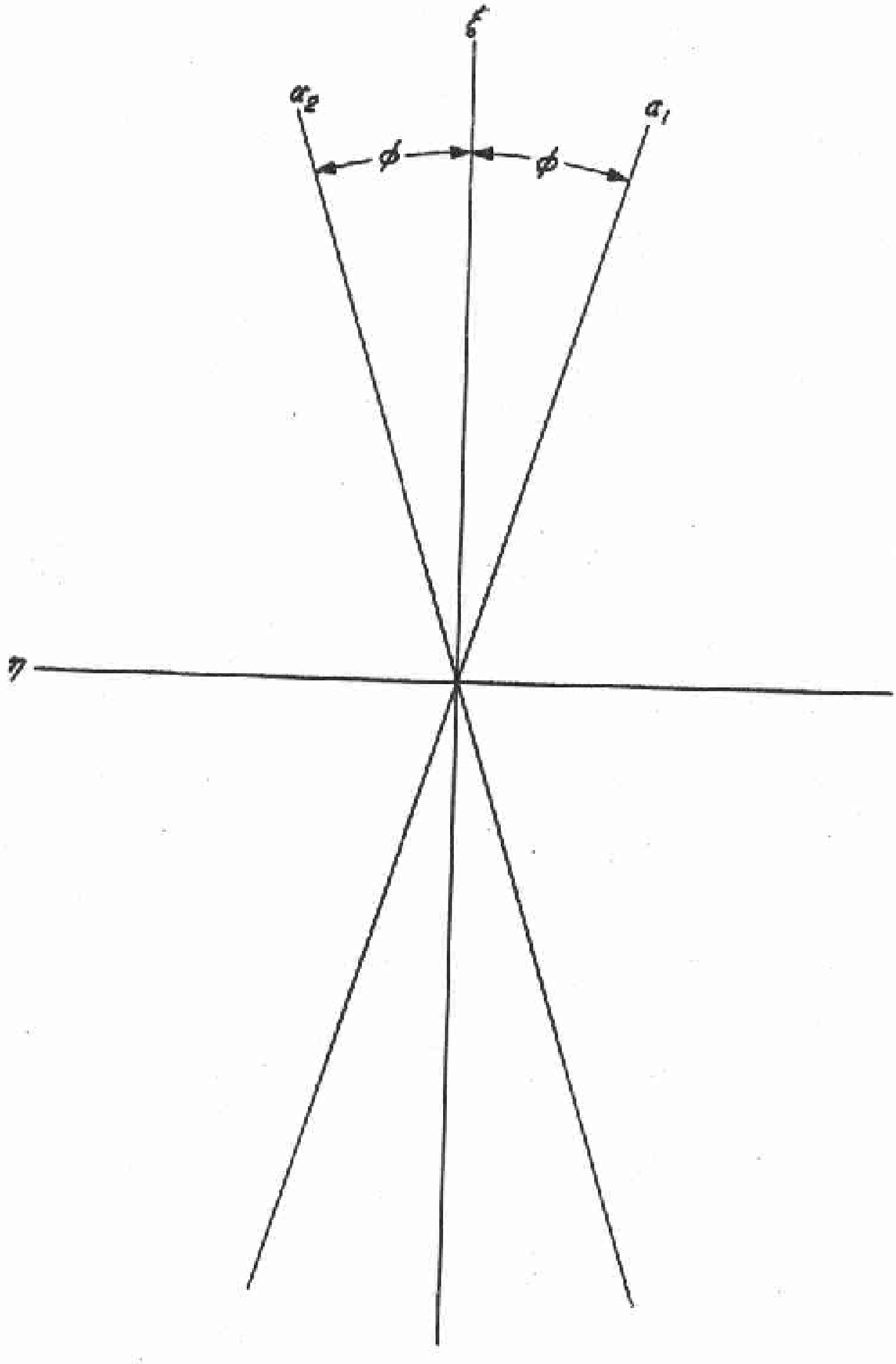

Figure 25. --Choice of axes for a laminate made of two identical orthotropic laminations.

Z M 106 681

SUBJECT LISTS OF PUBLICATIONS ISSUED BY THE FOREST PRODUCTS LABORATORY

The following are obtainable free on request from the Director, Forest Products Laboratory, Madison, Wisconsin 53705.

List of publications on
Box and Crate Construction
and Packaging Data

List of publications on
Chemistry of Wood and
Derived Products

List of publications on
Fire Protection

List of publications on
Fungus and Insect Defects
in Forest Products

List of publications on
Glue, Glued Products, and
Veneer

List of publications on
Growth, Structure, and
Identification of Wood

List of publications on
Logging, Milling, and Utilization of Timber Products

Partial list of publications for
Architects, Builders, Engineers,
and Retail Lumbermen

List of publications on
Mechanical Properties and
Structural Uses of Wood
and Wood Products

List of publications on
Pulp and Paper

List of publications on
Seasoning of Wood

List of publications on
Structural Sandwich, Plastic
Laminates, and Wood-Base
Aircraft Components

List of publications on
Thermal Properties of Wood

List of publications on
Wood Finishing

List of publications on
Wood Preservation

Partial list of publications for
Furniture Manufacturers,
Woodworkers, and Teachers
of Woodshop Practice

Note: Since Forest Products Laboratory publications are so varied in subject no single list is issued. Instead a list is made for each Laboratory division. Twice a year, December 31 and June 30, a list is made showing new reports for the previous 6 months. This is the only item sent regularly to the Laboratory's mailing list. Anyone who has asked for and received the proper subject lists and who has had his name placed on the mailing list can keep up to date on Forest Products Laboratory publications. Each subject list carries descriptions of all other subject lists.